Chapter 5: Synthesis and evaluation of multitargeted anti-Alzheimer's agent derived from 4-oxo-N, 4-diphenyl-butanamides and (E)-N-aryl-4-hydroxy-4-phenylbut-2-enamides

5.1 Introduction

Monoamine oxidase (MAO), exists in two isoenzymes, MAO-A and MAO-B, both are found in neurons and astroglia, coded by two distinct gene loci [1], with different distribution patterns inside the tissue. There are four highly conserved regions in MAO: a) ADP binding β-α-β unit (residues 6–43); b) putative substrate-binding domain (residues 178–221); c) flavin adenine dinucleotide (FAD) covalent attachment site (residues 380–458); and d) C terminus region (residues 491–511) predicted to form transmembrane-associated α-helix [2]. The volume of human MAO-A cavity (~400$Å^3$) is smaller than MAO-B (~700 $Å^3$) due to the presence of two different area, entrance cavity (~300$Å^3$) and substrate binding active site (~400$Å^3$) [3].

MAO inhibitors have also been proposed as potential neuroprotective and neurorescue agents as they preventing formation of neurotoxic by-products, *i.e*., hydrogen peroxide, toxic aldehydes, and hydroxyl free radicals. MAO-B has been reported to decrease the levels of the monoamines dopamine, norepinephrine, and serotonin in the brains of AD patients compared with healthy aging brain [4]. It is up-regulated, by up to 3-folds, in the temporal and frontal cortex associated with gliosis in AD, which can develop higher levels of H_2O_2 and oxidative free radicals [5]. The 5-hydroxytryptamine (5-HT) is a typical MAO-A substrate, whereas benzylamine and 2-phenylethylamine (PEA) are MAO-B substrates. Clorgyline and moclobemide are two selective MAO-A inhibitors, while R-(s)-deprenyl (selegiline), rasagiline, and lazabemide are selective MAO-B inhibitors (**Figure 5.1**).

Currently, the approved therapy for AD is only based on the reduction of cognitive disorder by intensifying cholinergic transmission through inhibition of acetylcholinesterase (AChE) and butyrylcholinesterase (BuChE). Tacrine, galanthamine, donepezil, and rivastigmine are the USFDA approved anti-AChE agents, to improve memory and cognitive function moderately in AD without affecting the progressive neurodegeneration [6]. Selegiline, a selective MAO-B inhibitor, has been reported to slow down the further deterioration of cognitive functions to more advanced stage [7]. The complexity of AD is unlikely that a single pharmacological activity will provide an exhaustive and adequate therapeutic approach. Single molecule with several pharmacological traits may work synergistically and is more likely to achieve the desired goal. The combined anti-AChE and anti-MAO activities in one molecular have been reported [8, 9]. MMP-2, -3, and -9 disrupt the blood-brain barrier, and might contribute to the formation and degradation of amyloid proteins in AD [10].

The fragment-based drug discovery assisted in designing 4-oxo-N, 4-diphenylbutanamides as dual MAO-B and AChE inhibitors. Modification at 4-oxo-butane motif of these provided E-N-aryl-4-hydroxy-4-phenylbut-2-enamides as more potent MAO-B inhibitors with AChE and matrix metalloproteinase-9 (MMP-9) inhibition.

The present study depicts preparation and preliminary *in vitro* screening of 4-oxo-N, 4-diphenylbutanamides, and E-N-aryl-4-hydroxy-4-phenylbut-2-enamides on MAO-B, cholinesterase and MMP-9 inhibition. Parallel artificial membrane permeability assay (PAMPA) has supported the blood-brain barrier (BBB) permeability of synthesized compounds. Significant cell viability and neuroprotectivity of the molecules support them to be considered as suitable AD drug candidates. In addition to the reduction in

oxidative stress, some compounds with MAO-A inhibitory activity may also have a direct effect on cognition and act as antidepressants

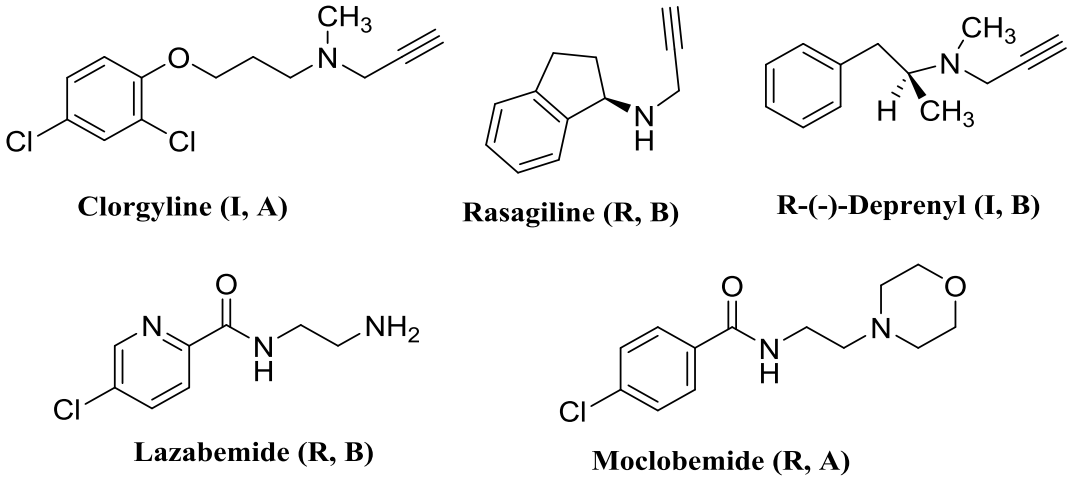

.

Figure 5.1. Irreversible (I), reversible (R), and selective MAO-A or MAO-B (A or B) inhibitors.

5.2 Materials and Methods

5.2.1 Fragment-based drug design

Fragment-based drug discovery facilitates the synthesized and screening of fewer compounds that are displaying a high success rate in developing chemical series with lead-like properties. Further, low-molecular-weight compounds (<250 AMU) target subpockets within the overall active site of MAO-B and AChE [11]. The binding interactions of these fragments with a target protein are weak, but they exhibit high ligand efficiency.

5.2.1.1 Protein structure preparation

The X-ray structures of human MAO-B and AChE, *i.e.,* 4A7A and 4M0E respectively, were collected from the Protein Data Bank (PDB) [12]. Protein structures were prepared and minimized, without any constraints inside the rigid protein, by using Protein Preparation Wizard in Maestro, Schrödinger.

5.2.1.2 Preparation of fragment database

All commercially available fragments were collected from various databases (*e.g.*, Zinc15, Asinex, and Cambridge) and database was prepared using LigPrep, Maestro. Out of these, fragments less than four rotatable bonds were selected for further studies.

5.2.1.3 Docking of fragments

The molecular docking was performed to screen large library against MAO-B and AChE separately. The docking poses corresponded closely to the crystallographic structures consequently determined by utilizing Glide, Maestro. Notably, these initial low-affinity hit(s) showed little specificity between MAO-B and AChE, which was unusual.

5.2.2 Molecular docking

Fragment based drug discovery provided '4-oxo-N, 4-diphenylbutanamide' as hit against MAO-B as well as AChE. All the possible modifications at 4-phenyl and N-phenyl moieties were designed and Glide XP docking was performed against MAO-B, MAO-A, and AChE using 4A7A, 2Z5Y, and 4M0E crystal structures respectively. The modification at '4-oxo-butanamide' motif of '4-oxo-N, 4-diphenylbutanamides' by '(E)-4-hydroxy but-2-enamide' afforded (E)-N-aryl-4-hydroxy-4-phenylbut-2-enamides, that were considered for molecular docking studies. N-Phenyl moiety was further replaced by N-quinolinyl (a 'zinc binding group' for MMP-9 inhibition) to design potent MAO-B and AChE inhibitors with MMP-9 inhibitory property.

5.2.3 Determination of drug-likeness

The drug-likeness properties of all the designed 4-oxo-N, 4-diphenylbutanamides and (E)-N-aryl-4-hydroxy-4-phenylbut-2-enamides were calculated using QikProp, Maestro.

All molecules were neutralized and minimized by utilizing LigPrep, Maestro, before calculation of physiochemical properties.

5.2.4 Organic chemistry

All chemicals and reagents were purchased from the Sigma-Aldrich, Avera, Spectrochem and Alfa Aesar for synthesis. The reactions were monitored by thin layer chromatography (TLC) on precoated silica gel 60 F254 plates (Merck KGaA) and spots were visualized under ultraviolet light (254 nm) or iodine vapors. Column chromatography was performed to purify the compounds by using silica gel (60-120 mesh size) as adsorbent and elution with appropriate solvents. Melting points were determined by using an automated melting point apparatus (Barnstead Electrothermal, UK). ^{1}H NMR and ^{13}C NMR spectra were recorded on Bruker Advance, 500 MHz spectrometer in DMSO-d_6. Chemical shifts (δ) were measured in ppm downfield from tetramethylsilane (TMS). Coupling constants (*J*) recorded in Hertz (Hz) and indicated apparent peak multiplications. Mass analyses were performed on the Q-ToF Micro Waters mass spectra with EI ion source. FTIR spectra were recorded on FTIR-8400S, Shimadzu, Japan. Purity of the synthesized compounds was determined by HPLC (Agilent Technologies 1260 infinity II LC System). An isocratic mobile phase composed of phase A (acetonitrile) and phase B (water) in the ratio of 9:1 was delivered by the binary pump with flow rate of 1ml/min. Samples were automatically injected into the HPLC column. CLC C^{18} column (5µ, 4.6 x 250 mm i.d, with CLC ODS, 4cm x 4.6 mm. i.d as guard column) with thermostatted column compartments (G1316A TCC) was used for analysis. Diode Array Detector WR was used at 250 nm for the detection of the compounds.

5.2.4.1 General procedure for the synthesis of (E)-4-Oxo-4-phenylbut-2-enoic acids (3a–e)

(E)-4-Oxo-4-phenylbut-2-enoic acids (**3a**–**e)** were synthesized by Friedel-Crafts acylation of substituted benzene (**2a**–**e**) (1 mmol) with maleic anhydride (**1**) (1 mmol) in presence of anhydrous $AlCl_3$ (2 mmol) as the catalyst, dry CH_2Cl_2 as solvent and excess of HCl formed was neutralised by $NaHCO_3$ (**Scheme 5.1**) [13]. After 3–5 h of stirring at 30–35 °C, the reaction mixture was captured with ice/HCl mixture. Solvent was removed under vacuum and excess substituted benzene was separated by steam distillation. Then the organic part was extracted by DCM and dried under vacuum. The Na_2CO_3 solution was added to the collected solids or oily substance and stirred, after basification, traces of aluminium from the catalyst was removed by filtration. The crude product was collected by neutralization with dropwise addition of HCl, and solid was washed thoroughly by water and dried. Final product was collected by recrystallized from suitable solvent (70–80% yield).

5.2.4.1.1 (E)-4-Oxo-4-phenylbut-2-enoic acids (3a)

Light orange crystals (74%), mp 92–93 °C; $C_{10}H_8O_3$; MW, 176.05; IR (ν, cm^{-1}): 1673.4 (C=C stretching), 1703.3 (C=O stretching); ^{1}H NMR (500 MHz, DMSO-d_6) δ: 11.62 (b, 1H), 8.01 (d, *J* = 6.74 Hz, 2H), 8.00 (d, *J* =15.73 Hz, 1H), 7.64 (t, *J* = 7.30 Hz, 1H), 7.51 (t, *J* = 7.86 Hz, 2H), 6.90 (d, *J* = 15.72 , 1H). ^{13}C NMR (125 MHz, DMSO-d_6) δ: 189.25, 170.77, 138.16, 136.14, 134.06, 131.44, 128.85.

5.2.4.1.2 (E)-4-(4-Methyl-phenyl)-4-oxo-but-2-enoic acids (3b)

Yellow crystals (75%), mp 138–139 °C; $C_{11}H_{10}O_3$; MW, 190.06; IR (ν, cm^{-1}): 1663.1, 1701.4; ^{1}H NMR (500 MHz, DMSO-d_6) δ: 11.62 (b,1H), 7.98 (d, *J* = 15.6 Hz, 1H), 7.90 (d, *J* = 8.2 Hz, 2H), 7.30 (d, *J* = 8.02 Hz, 2H), 6.86 (d, *J* = 15.45 Hz, 1H), 2.42 (s, 3H).

^{13}C NMR (125 MHz, DMSO-d_6) δ: 188.42, 170.58, 145.06, 138.32, 133.68, 130.93, 129.48, 128.91, 21.67.

*5.2.4.1.3 (***E***)-4-(4-Chloro-phenyl)-4-oxo-but-2-enoic acids (3c)*

Light yellow powder (89 %); mp 154–156 °C; $C_{10}H_7ClO_3$; MW, 210.0; IR (ν, cm^{-1}): 1676.2, 1705.08; ^{1}H NMR (500 MHz, DMSO-d_6) δ: 7.84 (d, *J* = 8.42 , 2H), 7.72 (d, *J* = 15.72 , 1H), 7.38 (d, *J* = 8.42 Hz, 2H), 6.74 (d, *J* = 15.16 Hz). ^{13}C NMR (125 MHz, DMSO-d_6) δ: 188.08, 166.49, 139.64, 134.49, 134.46, 133.44, 129.70, 128.66.

5.2.4.1.4 (E)-4-(4-Hydroxy-phenyl)-4-oxo-but-2-enoic acids (3d)

It was synthesised by the Friedel-Crafts acylation for 4 h and then followed the Fries rearrangement for 2 h at 70 °C. Yellow crystal (78%); mp 127–128 °C; $C_{10}H_8O_4$; MW, 192.17; IR (ν, cm^{-1}): 1672.1, 1701.6; ^{1}H NMR (500 MHz, DMSO-d_6) δ: 11.21 (b, 1H), 9.69 (s, 1H), 8.05 (d, *J* = 8.91 Hz, 2H), 8.08 (d, *J* = 15.41 Hz, 1H), 6.77 (d, *J* = 8.82 Hz, 2H), 6.87 (d, *J* = 15.41 Hz, 1H). ^{13}C NMR (125 MHz, DMSO-d_6) δ: 189.57, 170.41, 164.45, 141.54, 131.44, 130.8, 129.82, 116.21.

5.2.4.1.5 (E)-4-(4-Methoxy-phenyl)-4-oxo-4-phenylbut-2-enoic acids (3e)

Dark yellow powder (72%); mp 139 °C; $C_{11}H_{10}O_4$; MW, 206.05; IR (ν, cm^{-1}): 1677.09, 1704.43; ^{1}H NMR (500 MHz, DMSO-d_6) δ: 9.29 (b, 1H), 8.01 (d, *J* = 8.90 Hz, 2H), 8.00 (d, *J* = 15.41 Hz, 1H), 6.97 (d, *J* = 8.81 Hz, 2H), 6.87 (d, *J* = 15.41 Hz, 1H), 3.88 (s, 3H). ^{13}C NMR (125 MHz, DMSO-d_6) δ: 187.50, 170.71, 164.45, 138.54, 131.44, 130.78, 129.42, 114.21, 55.57.

5.2.4.2 General procedure for the synthesis of (E)-4-hydroxy-4-phenylbut-2-enoic acids (4a–e)

(E)-4-Oxo-4-phenylbut-2-enoic acids (**3a–e)** (1 mmol) were dissolved in 10% $NaHCO_3$ solution, sodium borohydride ($NaBH_4$) (1.1 mmol) was added at 4 °C, and stirred at room temperature for 2–4 h (**Scheme 5.1**) [14]. The mixture was acidified with 6N HCl

solution in cold condition and extracted with ethyl acetate. The combined extracts were dried by sodium sulfate, and evaporated in vacuum. Finally, pure (E)-4-hydroxy-4-phenylbut-2-enoic acids (**4a**–**e**) were obtained from recrystalization (70–90% yield).

5.2.4.2.1 (±) (E)-4-Hydroxy-4-phenylbut-2-enoic acids (4a)

Dark yellow powder (72%); mp 92–94 °C; $C_{10}H_{10}O_3$; MW, 178.19; IR (ν, cm^{-1}): 3467.28 (OH stretching), 1704.5 (C=O stretching); ^{1}H NMR (500 MHz, DMSO-d_6) δ 7.38 (s, 5H), 6.87 (d, 1H), 6.04 (d, 1H, *J* = 15 Hz), 5.30 (d, 1H, *J* =2.4 Hz, *J* =4.8 Hz), 8.1 (b, s, exch. D_2O, OH); ^{13}C NMR (125 MHz, DMSO-d_6) δ 171.6, 147.8, 142.02, 127.8, 128.9, 127.9, 121.5, 72.7.

5.2.4.2.2 (±) (E)-4-Hydroxy-4-(4-methyl-phenyl)but-2-enoic acids (4b)

Yellow powder (75%); mp 137–139 °C; $C_{11}H_{12}O_3$; MW, 192.21; IR (ν, cm^{-1}): 3467.8, 1700.78; ^{1}H NMR (500 MHz, DMSO-d_6) δ 7.72 (d, 1H, *J* =12.4 Hz), 7.23 (d, 2H, *J* = 8.9 Hz), 7.09 (d, 2H, *J* = 7.4 Hz), 5.97 (d, 1H, *J* = 15 Hz), 5.60 (d, 1H, *J* =2.4 Hz, *J* = 4.8 Hz), 2.24 (s, 3H), 8.9 (b, s, exch. D_2O, OH); ^{13}C NMR (125 MHz, DMSO-d_6) δ 171.5, 147.3, 142.02, 138.4, 137.7, 129.4, 121.2, 72.3, 27.2.

5.2.4.2.3 (±) (E)-4-(4-Chloro-phenyl)-4-hydroxy-but-2-enoic acids (4c)

Yellow powder (73%); mp 155–157 °C; $C_{10}H_9ClO_3$; MW, 212.6; IR (ν, cm^{-1}): 3468.3, 1700.21; ^{1}H NMR (500 MHz, DMSO-d_6) δ 7.39 (d, 2H), 7.27 (d, 1H), 6.04 (d, 1H, *J* = 15 Hz), 5.58 (d, 1H, *J* = 2.4 Hz, *J* =4.8 Hz), 10.9 (b, s, exch. D_2O, OH); ^{13}C NMR (125 MHz, DMSO-d_6) δ 171.5, 147.4, 139.8, 133.02, 129.5, 127.2, 121.1, 72.4.

5.2.4.2.4 (±) (E)-4-(4-Hydroxy-phenyl)-4-hydroxy-4-but-2-enoic acids (4d)

Yellowish brown powder (75%); mp 128–129 °C; $C_{10}H_{10}O_4$; MW, 194.19; IR (ν, cm^{-1}): 3467.8, 1700.1; ^{1}H NMR (500 MHz, DMSO-d_6) δ 7.17(d, 2H), 6.7(d, 2H), 6.87 (d, 1H), 6.04 (d, 1H, *J* = 15 Hz), 5.56 (d, 1H, *J* = 2.4 Hz, *J* = 4.8 Hz), 9.1 (b, s, exch. D_2O, OH),

8.9 (b, s, exch. D_2O, OH); ^{13}C NMR (125 MHz, DMSO-d_6) δ 171.5, 157.6, 147.3, 134.2, 129.5, 121.1, 116.1, 72.6.

5.2.4.2.5 (±) (E)-4-(4-Methoxy-phenyl)-4-hydroxy-4-but-2-enoic acids (4e)

Yellow powder (75%); mp 140–141 °C; $C_{11}H_{12}O_4$; MW, 208.21; IR (ν, cm^{-1}): 3468.7, 1702.8; ^1H NMR (500 MHz, DMSO-d_6) δ 7.72 (d, 1H, *J* = 2.4 Hz, *J* =4.8 Hz), 7.31 (d, 2H), 6.89 (d, 2H), 6.1 (d, 1H, *J* = 15 Hz), 5.90 (d, 1H, *J* = 8.8 Hz), 3.9 (s, 3H), 9.7 (b, s, exch. D_2O, OH); ^{13}C NMR (125 MHz, DMSO-d_6) δ 171.9, 147.4, 159.22, 133.9, 129.4, 121.8, 114.6, 72.8, 55.9.

Scheme 5.1 Synthesis of 4-oxo-N, 4-diphenylbutanamides (**6a**–**s**)

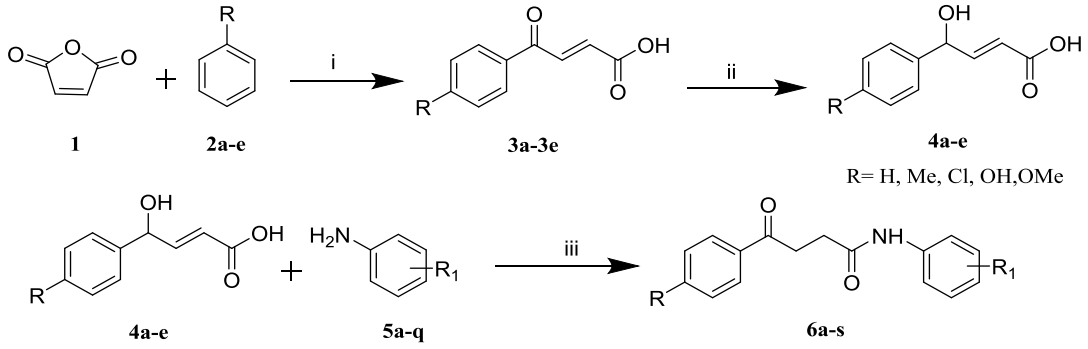

	R	R_1
6a	H	H
6b	H	4-Cl
6c	H	3-Cl
6d	H	4-Me
6e	H	4-OMe

	R	R_1
6f	H	3-OMe
6g	H	4-CF_3
6h	H	3-CF_3
6i	H	4-CN
6j	H	3-CN

	R	R_1
6k	H	3-COMe
6l	H	3,5-Me
6m	H	4-COMe
6n	H	4-OH
6o	H	2-OMe, 4-NO_2

	R	R_1
6p	OH	4-COMe
6q	Cl	4-COMe
6r	Me	4-Cl
6s	Me	3-F

Reagents and conditions: i) $AlCl_3$, dry DCM, stirred, 30–35 °C, 3–5 h, yield 70–80%. ii) Sodium borohydride, $NaHCO_3$, rt, stirring, 2–4 h, yield 70–90%. iii) 1-Ethyl-3-(3-dimethylaminopropyl)carbodiimide and hydroxybenzotriazole, ACN, rt, 6–8 h, yield 55–77%.

5.2.4.3 Procedure for the synthesis of 4-oxo-N, 4-diphenylbutanamides (6a–s)

(E)-4-Hydroxy-4-phenylbut-2-enoic acids (**4a**–**e**) (1 mmol) and different substituted amines (**5a**–**p**) (1 mmol) were dissolved in acetonitrile and stirred at room temperature for 6–8 h in presence of hydroxybenzotriazole (1.4 mmol) and 1-ethyl-3-(3-dimethylaminopropyl) carbodiimide (1.5 mmol) (**Scheme 5.1**). The solvent was evaporated in vacuum after the completion of reaction and extracted with

dichloromethane. Extract was dried with sodium sulphate and then the solvent was evaporated in vacuum to obtain the crude product. The product, 4-oxo-N, 4-diphenylbutanamides (**6a**–**s**), was purified by column chromatography using silica gel of 60–120 mesh as the stationary phase and ethyl acetate with hexane as mobile phase (yield 55–77%).

Plausible mechanism of synthesis of 4-oxo-N, 4-diphenylbutanamides from (E)-4-hydroxy-4-phenylbut-2-enoic acid is pictured in **Figure 5.2**. In this procedure, (±) (E)-N-aryl-4-hydroxy-4-phenylbut-2-enamides (**7a**–**x**) were also separated as minor products (yield 20–40%).

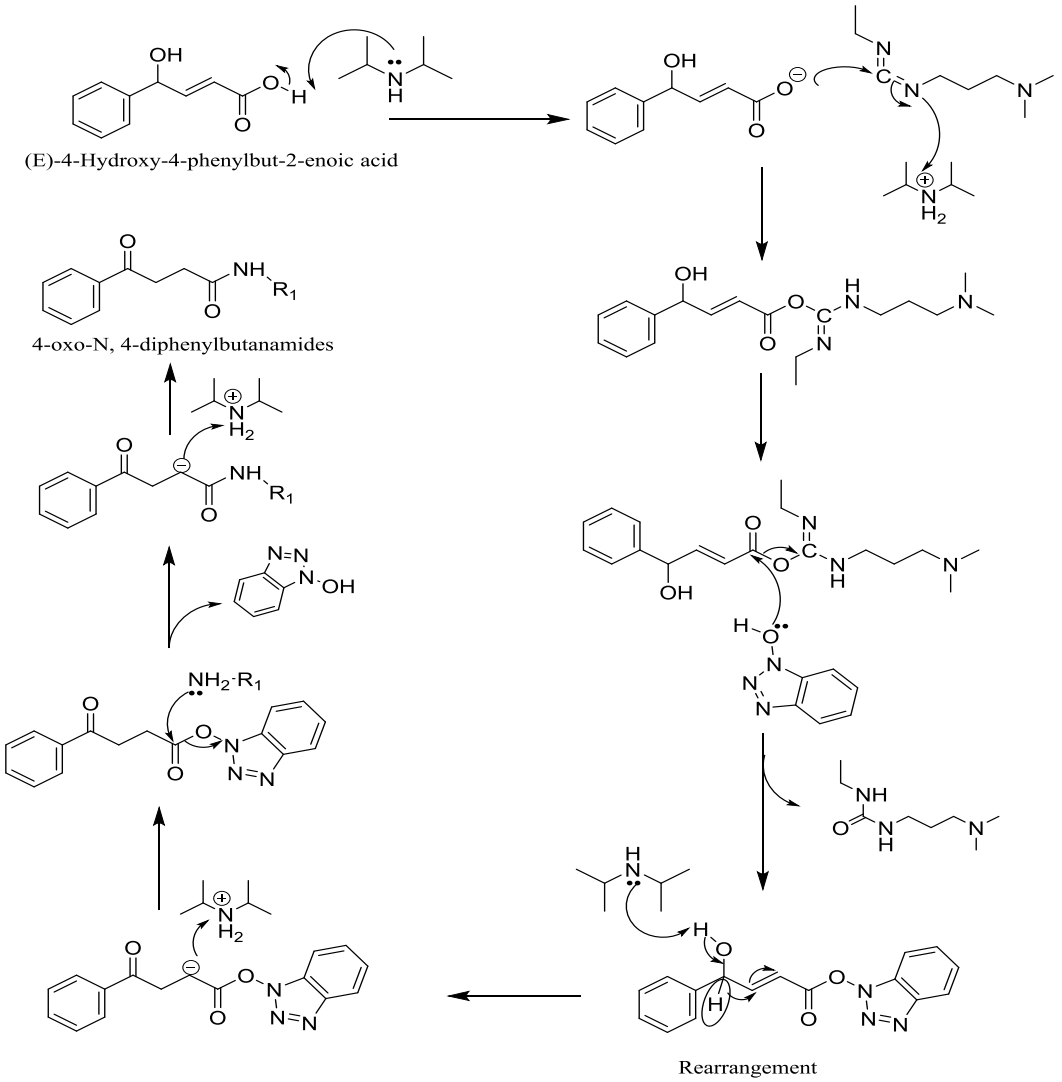

Figure 5.2 Plausible mechanism of 4-oxo-N, 4-diphenylbutanamides synthesis from (E)-4-hydroxy-4-phenylbut-2-enoic acid

4-Oxo-4-phenylbutanoic acids (1 mmol) also produced 4-oxo-N, 4-diphenyl butanamides (**6a**–**s**) with different substituted amines (**5a**–**p**) (1 mmol) on acetonitrile in presence of hydroxybenzotriazole (1.4 mmol) and 1-ethyl-3-(3-dimethylaminopropyl) carbodiimide (1.5 mmol) with stirring at room temperature for 8 h [15].

5.2.4.3.1 4-Oxo-N, 4-diphenylbutanamide (6a)

Yellow solid (68%); mp 286–288 ºC; $C_{16}H_{15}NO_2$; MW, 253.30; MS (ESI): *m/z*: found 253.05 [M^+], calc. 253.3; IR (ν, cm^{-1}): 3352.18 (NH stretching), 1703.20 (C=O stretching), 1672.34 (Ar CH stretching); ^{1}H NMR (500 MHz, DMSO-d6) δ 8.04− 7.94 (m, 2H), 7.83 (s, 1H), 7.60−7.45 (m, 5H), 7.30 (t, *J* = 7.8 Hz, 2H), 7.08 (t, *J* = 7.4 Hz, 1H), 3.46 (t, *J* = 6.4 Hz, 2H), 2.82 (t, *J* = 6.2 Hz, 2H); ^{13}C NMR (125 MHz, DMSO-d6) δ 199.3, 170.4, 138.0, 136.3, 133.4, 128.9, 128.6, 128.1, 124.1, 119.7, 34.1, 31.4.

5.2.4.3.2 N-(4-Chlorophenyl)-4-oxo-4-phenylbutanamide (6b)

Light brown (67%); mp 305–307 ºC; $C_{16}H_{14}ClNO_2$; MW, 287.75; MS (ESI): *m/z*: found 289.45 [M^{+2}], calc. 289.75. IR (ν, cm^{-1}): 3352.08, 1703.27, 1672.24; ^{1}H NMR (500 MHz, DMSO-d6) δ 10.18 (s, 1H), 8 (d, *J* =5 Hz, 2H), 7.63 (t, *J* =12.5 Hz, 3H), 7.54 (t, *J* = 7.5 Hz, 2H), 7.34 (d, *J* = 2.5 Hz, 2H), 2.73 (t, *J* = 7.5 Hz, 2H); ^{13}C NMR (125 MHz, DMSO-d6) δ 199.36, 171.06, 138.82, 137.03, 133.73, 129.18, 128.40, 126.91, 120.92, 33.58, 30.78.

5.2.4.3.3 N-(3-Chlorophenyl)-4-oxo-4-phenylbutanamide (6c)

Light orange (63%); mp 301–304 °C; $C_{16}H_{14}ClNO_2$; MW, 287.75; MS (ESI): *m/z*: found 289.05 [M^{+2}], calc. 289.75; IR (ν, cm^{-1}): 3352.02, 1703.26, 1672.84; ^{1}H NMR (500 MHz, DMSO-d6) δ 10.26 (s, 1H), 8.01 (d, *J* = 7.4 Hz, 2H), 7.82 (s, 1H), 7.66 (t, *J* = 7.1 Hz, 1H), 7.55 (t, *J* = 7.3 Hz, 2H), 7.44 (d, *J* = 8.0 Hz, 1H), 7.32 (t, *J* = 8.0 Hz, 1H), 7.08 (d, *J* = 7.8 Hz, 1H), 2.74 (t, *J* = 5.6 Hz, 2H); ^{13}C NMR (125 MHz, DMSO-d6)

δ 199.28, 171.30, 136.95, 133.70, 133.50, 130.88, 129.21, 128.34, 123.07, 118.79, 117.69, 33.47, 30.76.

5.2.4.3.4 4-Oxo-4-phenyl-N-(p-tolyl) butanamide (6d)

Yellow solid (69%); mp 289–291 °C; $C_{17}H_{17}NO_2$; MW, 267.33; MS (ESI): *m/z*: found 267.14 [M^+], calc. 267.33; IR (ν, cm^{-1}): 3352.68, 1703.22, 1672.34; ^{1}H NMR (500 MHz, DMSO-d6) δ 9.93 (s, 1H), 7.99 (t, *J* = 2.5 Hz, 2H), 7.64 (d, *J* = 5 Hz, 1H), 7.54 (t, *J* = 7.5 Hz, 2H), 7.27 (d, *J* = 5 Hz, 2H), 7.07 (d, *J* = 2.5 Hz, 2H), 2.7 (t, *J* = 5 Hz, 2H), 2.23 (s, 3H); ^{13}C NMR (125 MHz, DMSO-d6) δ 199.42, 170.57, 137.58 – 137.43, 137.25, 133.68, 132.21, 129.55, 129.24, 128.39, 119.41, 33.66, 30.73.

5.2.4.3.5 N-(4-Methoxyphenyl)-4-oxo-4-phenyl butanamide (6e)

Brownish white crystal (73%); mp 290–293 °C; $C_{17}H_{17}NO_3$; MW, 283.33; MS (ESI): *m/z*: found 283.15 [M^+], calc. 283.33; IR (ν, cm^{-1}): 3352.68, 1703.32, 1672.73; ^{1}H NMR (500 MHz, DMSO-d6) δ 10.5 (s, 1H), 8.02 (d, *J*=5.7 Hz, 2H), 7.62 (d, *J*=5.4 Hz, 2H), 7.15 (t, *J* = 7.5 Hz, 1H), 7.34 (d, *J* = 2.5 Hz, 2H), 7.18 (t, *J* = 9.5 Hz, 1H), 3.81 (s, 3H), 3.17 (t, *J* = 2.5 Hz, 2H), 2.71 (t, *J* = 5 Hz, 2H); ^{13}C NMR (125 MHz, DMSO-d6) δ 198.66, 177.6, 158.2, 137.35, 133.8, 130.4, 129.5, 128.04, 123.8, 114.15, 62.4, 37.8, 32.4.

5.2.4.3.6 N-(3-Methoxyphenyl)-4-oxo-4-phenyl butanamide (6f)

Yellow crystal (69%); mp 290–293 °C; $C_{17}H_{17}NO_3$; MW, 283.33; MS (ESI): *m/z*: found 283.12 [M^+], calc. 283.33; IR (ν, cm^{-1}): 3352.60, 1703.31, 1672.03; ^{1}H NMR (500 MHz, DMSO-d6) δ 10.02 (s, 1H), 8.05 (d, *J* = 5.3 Hz, 2H), 7.64 (d, *J* =5.0 Hz, 1H), 7.55 (t, *J* = 7.5 Hz, 2H), 7.31 (d, *J* = 2.5 Hz, 1H), 7.18 (t, *J* = 7.5 Hz, 1H), 6.6 (d, *J* = 2.5 Hz, 1H), 3.71 (s, 3H), 3.17 (t, *J* = 2.5 Hz, 2H), 2.71 (t, *J* = 5 Hz, 2H); ^{13}C NMR (125 MHz,

DMSO-d6) δ 198.66, 170.21, 159.31, 140.35, 136.35, 132.99, 129.25, 128.54, 127.68, 110.97, 108.15, 104.46, 32.88, 30.10.

5.2.4.3.7 4-Oxo-4-phenyl-N-(4-(trifluoromethyl)phenyl) butanamide (6g)

Light brown solid (67%); mp 290–293 °C; $C_{17}H_{14}F_3NO_2$; MW, 321.3; MS (ESI): *m/z*: found 321.07 [M^+], calc. 321.3; IR (ν, cm^{-1}): 3352.12, 1703.29, 1672.62; ^{1}H NMR (500 MHz, DMSO-d6) δ 10.44 (s, 1H), 8.01 (d, *J* = 6.9 Hz, 2H), 7.80 (d, *J* = 7.7 Hz, 2H), 7.66 (d, *J* = 6.9 Hz, 3H), 7.56 (d, *J* = 6.8 Hz, 2H), 2.78 (s, 2H); ^{13}C NMR (125 MHz, DMSO-d6) δ 199.26, 171.58, 143.34, 136.94, 133.71, 129.21, 128.35, 126.50, 119.18, 33.46, 30.83.

5.2.4.3.8 4-Oxo-4-phenyl-N-(3-(trifluoromethyl) phenyl) butanamide (6h)

Light yellow crystal (71%); mp 287–289 °C; $C_{17}H_{14}F_3NO_2$; MW, 321.3; MS (ESI): *m/z*: found 321.27 [M^+], calc. 321.3; IR (ν, cm^{-1}): 3352.86, 1703.29, 1672.04; ^{1}H NMR (500 MHz, DMSO-d6) δ 10.42 (s, 1H), 8.11 (s, 1H), 8.01 (d, *J* = 7.3 Hz, 2H), 7.75 (d, *J* = 7.8 Hz, 1H), 7.65 (d, *J* = 6.9 Hz, 1H), 7.56 (d, *J* = 6.5 Hz, 3H), 7.38 (d, *J* = 7.3 Hz, 1H), 2.76 (s, 2H); ^{13}C NMR (125 MHz, DMSO-d6) δ 199.26, 171.53, 133.72, 130.44, 129.22, 128.35, 122.83, 33.45, 30.74.

5.2.4.3.9 N-(4-Cyanophenyl)-4-oxo-4-phenylbutanamide (6i)

Orange solid (69%); mp 301–304 °C; $C_{17}H_{14}N_2O_2$; MW, 278.31; MS (ESI): *m/z*: found 278.29 [M^+], calc. 278.31; IR (ν, cm^{-1}): 3352.81, 1703.07, 1672.19; ^{1}H NMR (500 MHz, DMSO-d6) δ 10.52 (s, 1H), 8.01 (d, *J* = 7.1 Hz, 2H), 7.77 (s, 4H), 7.65 (d, *J* = 6.4 Hz, 1H), 7.55 (t, *J* = 6.2 Hz, 2H), 2.78 (s, 2H); ^{13}C NMR (125 MHz, DMSO-d6) δ 199.21, 171.80, 143.96, 136.90, 133.76, 129.22, 128.35, 127.40, 126.59, 105.06, 33.43, 30.91.

5.2.4.3.10 N-(3-Cyanophenyl)-4-oxo-4-phenylbutanamide (6j)

Yellow solid (68%); mp 291–293 °C; $C_{17}H_{14}N_2O_2$; MW, 278.31; MS (ESI): *m/z*: found 278.33 [M^+], calc. 278.31; IR (ν, cm^{-1}): 3352.03, 1703.46, 1672.29; ^{1}H NMR (500 MHz, DMSO-d6) δ 10.43 (s, 1H), 8.09 (s, 1H), 8.01 (d, *J* = 7.4 Hz, 2H), 7.80 (d, *J* = 7.6 Hz, 1H), 7.66 (d, *J* = 6.6 Hz, 1H), 7.53 (dt, *J* = 22.4, 7.4 Hz, 4H), 2.76 (s, 2H); ^{13}C NMR (125 MHz, DMSO-d6) δ 199.22, 171.59, 140.56, 136.92, 133.72, 130.73, 129.18, 128.35, 126.95, 126.59, 123.86, 121.90, 119.22, 112.00, 33.44, 30.75.

5.2.4.3.11 N-(3-Acetylphenyl)-4-oxo-4-phenylbutanamide (6k)

Brown crystal (71%); mp 311–313 °C; $C_{18}H_{17}NO_3$; MW, 295.34; MS (ESI): *m/z*: found 295.18 [M^+], calc. 295.34; IR (ν, cm^{-1}): 3352.60, 1713.29, 1703.31, 1672.03; ^{1}H NMR (500 MHz, DMSO-d6) δ 10.03 (s, 1H), 8.14 (s, 1H), 7.96 (d, *J* = 5.2 Hz, 2H), 7.8 (d, *J* = 2.5 Hz, 1H), 7.71 (d, *J* = 2.5 Hz, 1H), 7.55 (t, *J* = 7.5 Hz, 2H), 7.68 (t, *J* = 6.3 Hz, 1H), 7.48 (t, *J* = 7.5 Hz, 1H), 3.47 (d, *J* = 2.5 Hz, 2H), 2.71 (t, *J* = 2.8 Hz, 2H), 3.61 (s, 3H); ^{13}C NMR (125 MHz, DMSO-d6) δ 198.66, 170.21, 159.31, 140.35, 136.35, 132.99, 129.25, 128.54, 127.68, 110.97, 108.15, 104.46, 32.88, 30.10.

5.2.4.3.12 N-(3,5-Dimethylphenyl)-4-oxo-4-phenylbutanamide (6l)

Brownish white crystal (66%); mp 281–283 °C; $C_{18}H_{19}NO_2$; MW, 281.35; MS (ESI): *m/z*: found 281.37 [M^+], calc. 281.35; IR (ν, cm^{-1}): 3351.95, 1703.92, 1672.75; ^{1}H NMR (500 MHz, DMSO-d6) δ 10.03 (s, 1H), 7.99(d, *J* = 6.8 Hz, 2H), 7.67 (t, *J* = 6.5 Hz, 1H), 7.54 (t, *J* = 5.4 Hz, 2H), 7.44 (s, 1H), 7.17 (s, 1H), 3.53 (t, *J* = 3.5 Hz, 2H), 2.7 (t, *J* = 4.5 Hz, 2H), 2.28 (s, 6H); ^{13}C NMR (125 MHz, DMSO-d6) δ 199.42, 177.57, 138.9, 138.58, 138.1, 136.5, 133.3, 129.15, 128.24, 126.39, 122,4, 35.66, 30.73, 24.2.

5.2.4.3.13 N-(4-Acetylphenyl)-4-oxo-4-phenylbutanamide (6m)

Brown crystal (69%); mp 319–321 °C; $C_{18}H_{17}NO_3$; MW, 295.34; MS (ESI): *m/z*: found 295.18 [M^+], calc. 295.34; IR (ν, cm^{-1}): 3352.03, 1711.09, 1703.12, 1672.93; ^{1}H NMR

(500 MHz, DMSO-d6) δ 10.2 (s, 1H), 8.08 (d, *J* = 5.1 Hz, 2H), 7.97 (d, *J* = 5.1 Hz, 2H), 7.75 (d, *J* = 5.5 Hz, 2H), 7.64 (t, *J* = 5.1 Hz, 1H), 7.55 (t, *J* = 7.5 Hz, 2H), 3.41 (s, 3H), 2.61 (t, *J* = 2.7 Hz, 2H), 2.47 (t, *J* = 2.3 Hz, 2H); ^{13}C NMR (125 MHz, DMSO-d6) δ 198.66, 197.2, 177.1, 149.3, 136.8, 136.05, 1333.4, 129.25, 128.54, 127.68, 121.47, 32.88, 30.11, 26.7.

5.2.4.3.14 N-(4-Hydroxyphenyl)-4-oxo-4-phenylbutanamide (6n)

Brown crystal (58%); mp 303–305 °C; $C_{16}H_{15}NO_3$; MW, 269.3; MS (ESI): *m/z*: found 269.26 [M^+], calc. 269.3; IR (ν, cm^{-1}): 3352.03, 1711.09, 1703.12, 1672.93; ^{1}H NMR (500 MHz, DMSO-d6) δ 10.04 (s, 1H), 9.4 (s, 1H), 8.0 (d, *J* = 5.8 Hz, 2H), 7.49 (d, *J* = 6.2 Hz, 1H), 7.72 (t, *J* = 5.4 Hz, 1H), 7.35 (d, *J* = 5.5 Hz, 2H), 6.6 (d, *J* = 5.5 Hz, 2H), 3.71 (t, *J* = 2.4 Hz, 2H), 2.51 (t, *J* = 5.3 Hz, 2H); ^{13}C NMR (125 MHz, DMSO-d6) δ 198.3, 177.4, 154.31, 136.5, 133.05, 131.19, 129.05, 128.4, 123.6, 116.07, 35.88, 30.91.

5.2.4.3.15 N-(2-Methoxy-4-nitrophenyl)-4-oxo-4-phenylbutanamide (6o)

Dark drown solid (66%); mp 318–320 °C; $C_{17}H_{16}N_2O_5$; MW, 328.32; MS (ESI): *m/z*: found 328.11 [M^+], calc. 328.32; IR (ν, cm^{-1}): 3352.03, 1711.09, 1703.12, 1672.93; ^{1}H NMR (500 MHz, DMSO-d6) δ 10.04 (s, 1H), 7.97 (d, *J* = 5.7 Hz, 2H), 7.9 (d, *J* = 5.4 Hz, 2H), 7.85 (d, *J* = 6.5 Hz, 1H), 7.68 (t, *J* = 6.5 Hz, 1H), 7.48 (t, *J* = 7.5 Hz, 2H), 3.91 (s, 3H), 3.47 (t, *J* = 2.5 Hz, 2H), 2.47 (t, *J* = 3.5 Hz, 2H); ^{13}C NMR (125 MHz, DMSO-d6) δ 198.36, 177.4, 154.9, 144.5, 136.75, 133.12, 132.99, 128.9, 128.54, 116.6, 112.7, 105.7, 55.9, 35.65, 30.54.

5.2.4.3.16 N-(4-Acetylphenyl)-4-(4-hydroxyphenyl)-4-oxobutanamide (6p)

Brown solid (67%); mp 323–325 °C; $C_{18}H_{17}NO_4$; MW, 311.34; MS (ESI): *m/z*: found 311.06 [M^+], calc. 311.34; IR (ν, cm^{-1}): 3352.03, 1711.09, 1703.12, 1672.93; ^{1}H NMR (500 MHz, DMSO-d6) δ 9.97 (s, 1H), 9.67 (s, 1H), 8.07 (d, *J* = 6.5 Hz, 2H), 7.78 (d, *J* = 6.1 Hz, 2H), 7.7 (d, *J* = 7.5 Hz, 2H), 6.76 (d, *J* = 7.5 Hz, 2H), 3.65 (t, *J* = 2.5 Hz, 2H),

2.71 (t, *J* = 5 Hz, 2H), 2.6 (s, 3H); ^{13}C NMR (125 MHz, DMSO-d6) δ 198.3, 197.2, 177.6, 162.9, 142.75, 136.7, 130.4, 129.5, 121.6, 115.8, 35.15, 30.4, 26.7.

5.2.4.3.17 N-(4-acetylphenyl)-4-(4-chlorophenyl)-4-oxobutanamide (6q)

Yellowish white crystal (76%); mp 305–307 °C; $C_{18}H_{17}NO_3$; MW, 329.78; MS (ESI): *m/z*: found 329.61 [M^+], calc. 329.78; IR (ν, cm^{-1}): 3352.03, 1711.09, 1703.12, 1672.93; ^{1}H NMR (500 MHz, DMSO-d6) δ 9.97 (s, 1H), 8.07 (d, *J* = 6.5 Hz, 2H), 7.9 (d, *J* = 6.1 Hz, 2H), 7.7 5(d, *J* = 7.5 Hz, 2H), 7.58 (d, *J* = 7.5 Hz, 2H), 3.65 (t, *J* = 2.5 Hz, 2H), 2.71 (t, *J* = 5 Hz, 2H), 2.52 (s, 3H); ^{13}C NMR (125 MHz, DMSO-d6) δ 198.4, 197.0, 177.4, 142.9, 138.7, 136.7, 134.3, 130.2, 129.6, 128.7, 121.8, 35.12, 30.1, 26.6.

5.2.4.3.18 N-(4-Chlorophenyl)-4-oxo-4-(p-tolyl)butanamide (6r)

Yellow white (67%); mp 302–304 °C; $C_{17}H_{16}ClNO_2$; MW, 301.77; MS (ESI): *m/z*: found 303.28 [M^{+2}], calc. 303.77; IR (ν, cm^{-1}): 3352.54, 1703.07, 1672.49; ^{1}H NMR (500 MHz, DMSO-d6) δ 10.13 (s, 1H), 7.85 (d, *J* = 7.9 Hz, 2H), 7.57 (d, *J* = 8.7 Hz, 2H), 7.30 (d, *J* = 6.5 Hz, 4H), 2.66 (t, *J* = 6.5 Hz, 2H), 2.34 (s, 3H); ^{13}C NMR (125 MHz, DMSO-d6) δ 198.83, 171.11, 144.05, 138.82, 134.56, 129.78, 129.10, 128.51, 126.89, 120.92, 33.45, 30.80.

5.2.4.3.19 N-(3-Fluorophenyl)-4-oxo-4-(p-tolyl)butanamide (6s)

Brownish yellow crystal (68%); mp 291–293 °C; $C_{17}H_{16}FNO_2$; MW, 285.32; MS (ESI): *m/z*: found 285.09 [M^+], calc. 285.32; IR (ν, cm^{-1}): 3352.78, 1703.28, 1672.04; ^{1}H NMR (500 MHz, DMSO-d6) δ 10.27 (s, 1H), 7.90 (d, *J* = 7.2 Hz, 2H), 7.59 (d, *J* = 11.6 Hz, 1H), 7.39 – 7.26 (m, 4H), 6.89 – 6.78 (m, 1H), 2.72 (t, *J* = 5.6 Hz, 2H), 2.39 (s, 3H); ^{13}C NMR (125 MHz, DMSO-d6) δ 198.75, 171.32, 130.82, 129.74, 128.46, 115.04, 33.35, 30.78.

5.2.4.4 General procedure for the synthesis of (E)-N-aryl-4-hydroxy-4-phenylbut-2-enamides (7a–x)

Different substituted amines (**5a**–**p**) (1 mmol) and (E)-4-Hydroxy-4-phenylbut-2-enoic acids (**4a**–**e**) (1 mmol) were dissolved in acetonitrile and stirred at room temperature in presence of triethylamine (4 mmol). Thionyl chloride (1 mmol) was added to it dropwise, and after 2 h reaction was completed (**Scheme 5.2**). The solvent was evaporated in vacuum after the completion of reaction and extracted with dichloromethane (DCM). Extract was dried with sodium sulphate and then the solvent was evaporated in vacuum to obtain the crude product. (E)-N-Aryl-4-hydroxy-4-phenylbut-2-enamides (7a–x) were purified by column chromatography using Silica gel of 60–120 mesh as the stationary phase and ethyl acetate with hexane as mobile phase (yield 60–75%).

Scheme 5.2 Synthesis of (E)-N-aryl-4-hydroxy-4-phenylbut-2-enamides (7a–x)

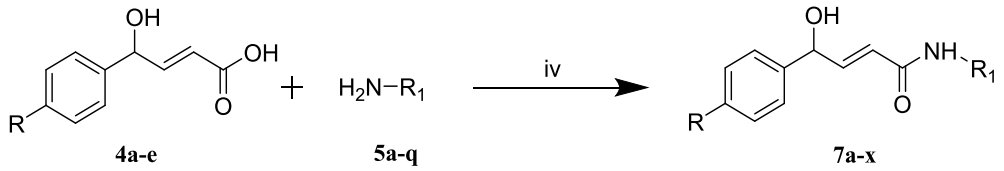

4a-e **5a-q** **7a-x**

	R	R_1		R	R_1		R	R_1		R	R_1
7a	H	Ph	7g	H	3-COMePh	7m	OH	4-ClPh	7s	OH	4-CF_3Ph
7b	H	3-ClPh	7h	H	3,5-MePh	7n	OH	4-MePh	7t	OH	4-OMePh
7c	H	4-MePh	7i	H	4-COMePh	7o	OH	4-NO_2Ph	7u	OH	3-CF_3Ph
7d	H	4-OMePh	7j	H	2-OMe, 4-NO_2Ph	7p	OH	6-Quinolinyl	7v	OH	4-COMePh
7e	H	3-CF_3Ph	7k	Me	4-OHPh	7q	OH	3-Quinolinyl	7w	OMe	6-Quinolinyl
7f	H	4-CNPh	7l	Cl	4-COMePh	7r	OH	8-Quinolinyl	7x	OMe	6-Quinolinyl

Reagents and conditions: iv) $SOCl_2$, Et_3N, ACN, rt, 2 h, yield 40–70%.

5.2.4.4.1 (±)(E) 4-Hydroxy-N, 4-diphenylbut-2-enamide (7a)

Yellow white (67%); mp 254–256 °C; $C_{16}H_{15}NO_2$; MW, 253.3; MS (ESI): *m/z*: found 253.27 [M^+], calc. 253.3; IR (ν, cm^{-1}): 3551.01 (OH stretching), 3350.54 (NH stretching), 1706.07 (C=O stretching), 1674.09 (C=C stretching); ^{1}H NMR (500 MHz, DMSO-d6) δ: 7.56 (d, *J* = 7.9 Hz, 2H), 7.34 (d, *J* = 8.7 Hz, 2H), 7.29 (t, *J* = 6.7 Hz,

1H), 7.28 (d, *J* = 6.5 Hz, 2H), 7.25 (d, *J* = 6.2 Hz, 2H), 7.07 (t, *J* = 6.7 Hz, 1H), 7.28 (t, *J* = 12.6 Hz, 1H), 7.22 (d, *J* = 12.6 Hz, 1H), 4.56 (d, *J* = 2.6 Hz, 1H), 10.13 (b, s, exch. D_2O, NH), 5.34 (b, s, OH); ^{13}C NMR (125 MHz, DMSO-d6) δ: 169.91, 143.6, 141.5, 140.2, 128.8, 128.01, 127.6, 127.1, 123.2, 121.92, 73.5.

5.2.4.4.2 (±)(E) N-(3-Chlorophenyl)-4-hydroxy-4-phenylbut-2-enamide (7b)

Light yellow (68%); mp 276–278 °C; $C_{16}H_{14}C_{l1}NO_2$; MW, 287.8; MS (ESI): *m/z*: found 289.14 [M^{+2}], calc. 289.8; IR (ν, cm^{-1}): 3551.01, 3350.54, 1706.07, 1674.09; ^1H NMR (500 MHz, DMSO-d6) δ: 7.9 (s, 1H), 7.69 (d, *J* = 8.7 Hz, 1H), 7.39 (t, *J* = 7.9 Hz, 1H), 7.33 (d, *J* = 6.7 Hz, 2H), 7.29 (t, *J* = 6.5 Hz, 1H), 7.28 (d, *J* = 6.7 Hz, 2H), 7.17 (d, *J*= 6.7 Hz, 1H), 7.28 (t, *J* =12.7 Hz, 1H), 7.21 (d, *J* =12.6 Hz, 1H), 5.57 (d, *J* =2.4 Hz, 1H), 9.3 (b, s, NH), 5.12 (b, s, OH); ^{13}C NMR (125 MHz, DMSO-d6) δ: 167.21, 143.5, 141.6, 137.6, 130.3, 128.9, 128.01, 127.9, 127.6, 127.1, 123.2, 122.01, 119.7, 72.5.

5.2.4.4.3 (±)(E) 4-Hydroxy-4-phenyl-N-(p-tolyl)but-2-enamide (7c)

Yellow crystal (71%); mp 263–265 °C; $C_{17}H_{17}NO_2$; MW, 267.3; MS (ESI): *m/z*: found 267.6 [M^+], calc. 267.3; IR (ν, cm^{-1}): 3551.01, 3350.54, 1706.07, 1674.09; ^1H NMR (500 MHz, DMSO-d6) δ: 7.56 (d, *J* = 7.9 Hz, 2H), 7.33 (d, *J* = 8.7 Hz, 2H), 7.29 (t, *J* = 7.7 Hz, 1H), 7.28 (d, *J* = 6.9 Hz, 2H), 7.17 (d, *J* = 7.2 Hz, 2H), 7.28 (t, *J* = 12.6 Hz, 1H), 7.22 (d, *J* = 13.1 Hz, 1H), 4.3 (d, *J* = 3.6 Hz, 1H), 2.37 (s, 3H), 9.26 (b, s, exch. D_2O, NH), 5.14 (b, s, OH); ^{13}C NMR (125 MHz, DMSO-d6) δ: 167.1, 141.6, 143.4, 136.8, 134.6, 129.4, 128.91, 127.6, 127.1, 123.06, 121.5, 72.2, 23.2.

5.2.4.4.4 (±)(E) 4-Hydroxy-N-(4-methoxyphenyl)-4-phenylbut-2-enamide (7d)

Light yellow crystal (67%); mp 287–289 °C; $C_{17}H_{17}NO_3$; MW, 283.3; MS (ESI): *m/z*: found 283.12 [M^+], calc. 283.3; IR (ν, cm^{-1}): 3551.01, 3350.54, 1706.07, 1674.09; ^1H NMR (500 MHz, DMSO-d6) δ: 7.71 (d, *J* = 7.9 Hz, 2H), 7.33 (d, *J* = 8.7 Hz, 2H), 7.29 (t, *J* = 6.7 Hz, 1H), 7.28 (d, *J* = 6.5 Hz, 2H), 6.97 (d, *J* = 6.2 Hz, 2H), 7.28 (t, *J* = 12.6

Hz, 1H), 7.22 (d, *J* = 13.1 Hz, 1H), 4.06 (d, *J* = 3.6 Hz, 1H), 3.86 (s, 3H), 10.13 (b, s, exch. D_2O, NH), 5.34 (b, s, OH); ^{13}C NMR (125 MHz, DMSO-d6) δ: 167.21, 158.9, 143.6, 141.5, 129.9, 128.8, 127.6, 127.1, 123.2, 122.6, 114.5, 723, 55.9.

5.2.4.4.5 (±)(E) 4-Hydroxy-4-phenyl-N(3-(trifluoromethyl)phenyl)but-2-enamide (7e)

Brownish white (71%); mp 264–266 °C; $C_{17}H_{14}F_3NO_2$; MW, 321.3; MS (ESI): *m/z*: found 321.26 [M^+], calc. 321.3; IR (ν, cm^{-1}): 3551.01, 3350.54, 1706.07, 1674.09; ^1H NMR (500 MHz, DMSO-d6) δ: 8.30 (s, 1H), 7.92 (d, *J* = 7.9 Hz, 1H), 7.62 (d, *J* = 8.7 Hz, 1H), 7.40 (t, *J* = 7.9 Hz, 1H), 7.28 (d, *J* = 6.5 Hz, 2H), 7.34 (d, *J* = 6.2 Hz, 2H), 7.29 (t, *J* = 8.7 Hz, 1H), 7.29 (d, *J* = 12.6 Hz, 1H), 7.21 (t, *J* = 12.8 Hz, 1H), 4.08 (d, *J* = 2.7 Hz, 1H), 9.26 (b, s, exch. D_2O, NH), 5.12 (b, s, OH); ^{13}C NMR (125 MHz, DMSO-d6) δ: 166.76, 143.3, 141.6, 139.7, 131.5, 131.2, 129.2, 128.8, 127.7, 127.1, 124.9, 124.2, 120.7, 116.9, 72.3.

5.2.4.4.6 (±)(E) N-(4-Cyanophenyl)-4-hydroxy-4-phenylbut-2-enamide (7f)

Orange crystal (69%); mp 283–285 °C; $C_{17}H_{14}N_2O_2$; MW, 278.3; MS (ESI): *m/z*: found 278.23 [M^+], calc. 279.3; IR (ν, cm^{-1}): 3551.01, 3350.54, 1706.07, 1674.09; ^1H NMR (500 MHz, DMSO-d6) δ: 7.83 (d, *J* = 7.6 Hz, 2H), 7.62 (d, *J* = 7.4 Hz, 2H), 7.33 (d, *J* = 7.7 Hz, 2H), 7.29 (t, *J* = 6.7 Hz, 1H), 7.28 (d, *J* = 7.5 Hz, 2H), 7.28 (d, *J* = 12.6 Hz, 1H), 7.22 (t, *J* = 13.1 Hz, 1H), 4.55 (d, *J* = 3.5 Hz, 1H), 9.2 (b, s, exch. D_2O, NH), 5.14 (b, s, OH); ^{13}C NMR (125 MHz, DMSO-d6) δ: 166.1, 143.3, 141.9, 141.4, 132.4, 128.8, 125.61, 125.5, 123.5, 123.02, 118.6, 116.0, 108.1, 72.4.

5.2.4.4.7 (±)(E) N-(3-Acetylphenyl)-4-hydroxy-4-phenylbut-2-enamide (7g)

Brownish white (72%); mp 307–309 °C; $C_{18}H_{17}NO_3$; MW, 295.3; MS (ESI): *m/z*: found 295.37 [M^+], calc. 295.3; IR (ν, cm^{-1}): 3551.01, 3350.54, 1706.07, 1674.09; ^1H NMR (500 MHz, DMSO-d6) δ: 8.12 (s.1H), 7.84 (d, *J* = 7.6 Hz, 1H), 7.77 (d, *J* = 7.5 Hz, 1H), 7.47 (t, *J* = 7.4 Hz, 1H), 7.33 (d, *J* = 8.7 Hz, 2H), 7.29 (t, *J* = 6.7 Hz, 1H), 7.28 (d, *J* =

6.5 Hz, 2H), 7.28 (d, *J* = 12.6 Hz, 1H), 7.22 (t, *J* = 13.1 Hz, 1H), 4.5 (d, *J* = 3.6 Hz, 1H), 3.2 (s, 3H), 9.3 (b, s, exch. D_2O, NH), 5.4 (b, s, OH); ^{13}C NMR (125 MHz, DMSO-d6) δ: 197.3, 167.5, 143.5, 141.5, 136.9, 135.9, 133.1, 128.9, 127.61, 127.1, 126.2, 124.4, 123.02, 118.4, 73.1, 26.7.

5.2.4.4.8 (±)(E) N-(3, 5-Dimethylphenyl)-4-hydroxy-4-phenylbut-2-enamide (7h)

Brownish white (74%); mp 284–286 °C; $C_{18}H_{19}NO_2$; MW, 281.4; MS (ESI): *m/z*: found 281.47 [M^+], calc. 281.4; IR (ν, cm^{-1}): 3551.01, 3350.54, 1706.07, 1674.09; ^1H NMR (500 MHz, DMSO-d6) δ: 7.5 (s, 2H), 7.33 (d, *J* = 8.7 Hz, 2H), 7.29 (t, *J* = 6.7 Hz, 1H), 7.28 (d, *J* = 8.7 Hz, 2H), 7.18 (s,1H), 7.2 (d, *J* = 12.3 Hz, 1H), 7.22 (t, *J* = 13.3 Hz, 1H), 4.16 (d, *J* = 2.6 Hz, 1H), 2.23 (s, 6H), 10.1 (b, s, exch. D_2O, NH), 5.34 (b, s, OH); ^{13}C NMR (125 MHz, DMSO-d6) δ: 166.1, 143.61, 141.5, 138.62, 135.71, 128.9, 127.9, 127.2, 126.6, 123.01, 122.6, 121.92, 73.1, 21.7.

5.2.4.4.9 (±)(E) N-(4-Acetylphenyl)-4-hydroxy-4-phenylbut-2-enamide (7i)

Brown crystal (69%); mp 311–313 °C; $C_{18}H_{17}NO_3$; MW, 295.3; MS (ESI): *m/z*: found 295.08 [M^+], calc. 295.3; IR (ν, cm^{-1}): 3551.01, 3350.54, 1706.07, 1674.09; ^1H NMR (500 MHz, DMSO-d6) δ: 8.07 (d, *J* = 7.6 Hz, 2H), 7.75 (d, *J* = 7.9 Hz, 2H), 7.34 (d, *J* = 8.9 Hz, 2H), 7.29 (t, *J* = 6.7 Hz, 1H), 7.28 (d, *J* = 7.4 Hz, 2H), 7.28 (t, *J* = 12.6 Hz, 1H), 7.22 (t, *J* = 13.1 Hz, 1H), 5.56 (d, *J* = 3.6 Hz, 1H), 3.1 (s,1H), 9.8 (b, s, exch. D_2O, NH), 5.84 (b, s, OH); ^{13}C NMR (125 MHz, DMSO-d6) δ: 197.2, 167.54, 143.4, 142.1, 141.6, 136.6, 129.1, 128.9, 127.6, 127.1, 123.2, 121.5, 72.5, 27.01.

5.2.4.4.10 (±)(E)4-Hydroxy-N-(2-methoxy-4-nitrophenyl)-4-phenylbut-2-enamide (7j)

Brown crystal (76%); mp 323–325 °C; $C_{17}H_{16}N_2O_5$; MW, 328.3; MS (ESI): *m/z*: found 328.07 [M^+], calc. 328.3; IR (ν, cm^{-1}): 3551.01, 3350.54, 1706.07, 1674.09; ^1H NMR (500 MHz, DMSO-d6) δ: 7.94 (s, 1H), 7.86 (d, *J* = 8.4 Hz, 1H), 7.9 (d, *J* = 7.7 Hz, 1H), 7.35 (d, *J* = 6.9 Hz, 2H), 7.29 (t, *J* = 7.5 Hz, 1H), 7.28 (d, *J*=6.6 Hz, 1H), 7.22 (t, *J* =

13.5 Hz, 1H), 6.19 (d, *J* = 13.2 Hz, 1H), 4.5 (d, *J* = 2.82 Hz, 1H), 3.87 (s, 3H), 10.03 (b, s, exch. D_2O, NH), 5.94 (b, s, OH); ^{13}C NMR (125 MHz, DMSO-d6) δ: 167.13, 154.9, 144.6, 143.5, 141.7, 130.4, 128.9, 127.6, 127.1, 123.2,116.4, 115.7, 105.5, 72.4, 55.8.

5.2.4.4.11 (±) (E) 4-Hydroxy-N-(4-hydroxyphenyl)-4-(p-tolyl) but-2-enamide (7k)

Yellow crystal (67%); mp 292–294 °C; $C_{17}H_{17}NO_3$; MW, 283.3; MS (ESI): *m/z*: found 283.04 [M^+], calc. 283.3; IR (ν, cm^{-1}): 3551.01, 3350.54, 1706.07, 1674.09; ^1H NMR (500 MHz, DMSO-d6) δ: 7.8 (d, *J* = 7.7 Hz, 2H), 7.6 (d, *J* = 8.2 Hz, 2H), 7.19 (t, *J* = 6.7 Hz, 1H), 6.75 (d, *J* = 7.5 Hz, 2H), 7.23 (t, *J* = 12.5 Hz, 1H), 7.21 (t, *J* = 12.7 Hz, 1H), 3.54 (d, *J* = 2.7 Hz, 1H), 1.8 (s, 3H), 12.6, (b, s, exch. D_2O, NH), 9.44 (b, s, OH), 5.12 (b, s, OH); ^{13}C NMR (125 MHz, DMSO-d6) δ: 167.1, 154.2, 143.6, 138.2, 137.3, 130.2, 129.3, 124.01, 123.6, 123.1, 116.2, 72.4, 21.3.

5.2.4.4.12 (±)(E) N-(4-Acetylphenyl)-4(4-chlorophenyl) 4-hydroxybut-2-enamide (7l)

Yellow white (68%); mp 311–313 °C; $C_{18}H_{16}C_{l1}NO_3$; MW, 329.8; MS (ESI): *m/z*: found 331.48 [M^{+2}], calc. 331.8; IR (ν, cm^{-1}): 3551.01, 3350.54, 1706.07, 1674.09; ^1H NMR (500 MHz, DMSO-d6) δ: 8.06 (d, *J* = 7.7 Hz, 2H), 7.75 (d, *J* = 8.2 Hz, 2H), 7.38 (d, *J* = 6.8 Hz, 2H), 7.22 (d, *J* = 7.5 Hz, 2H), 7.23 (d, *J* = 12.2 Hz, 1H), 7.07 (t, *J* = 12.7 Hz, 1H), 4.06 (d, *J* = 2.6 Hz, 1H), 2.51 (s, 3H), 10.17 (b, s, exch. D_2O, NH), 5.04 (b, s, OH); ^{13}C NMR (125 MHz, DMSO-d6) δ: 198.1, 167.1, 143.16, 142.01, 139.6, 136.7, 133.2, 129.1, 128.8, 127.1, 123.2, 121.5, 73.5, 26.7.

5.2.4.4.13 (±)(E) N-(4-Chlorophenyl)-4-hydroxy-4-(4-hydroxyphenyl)but-2-enamide (7m)

Yellow solid (58%); mp 302–304 °C; $C_{16}H_{14}C_{l1}NO_3$; MW, 303.8; MS (ESI): *m/z*: found 305.07 [M^{+2}], calc. 305.8; IR (ν, cm^{-1}): 3551.01, 3350.54, 1706.07, 1674.09; ^1H NMR (500 MHz, DMSO-d6) δ: 7.87 (d, *J* = 7.7 Hz, 2H), 7.40 (d, *J* = 8.3 Hz, 2H), 7.11 (d, *J* = 6.7 Hz, 2H), 6.74 (d, *J* = 6.9 Hz, 2H), 7.22 (t, *J* = 13.4 Hz, 1H), 7.1 (d, *J* = 12.9 Hz,

1H), 4.6 (d, *J* = 3.6 Hz, 1H), 10.01 (b, s, exch. D_2O, NH), 9.01 (b, s, OH), 5.04 (b, s, OH); ^{13}C NMR (125 MHz, DMSO-d6) δ: 167.01, 157.7, 143.6, 135.7, 134.3, 133.2, 129.6, 129.0, 123.12, 121.7, 116.2, 73.01.

5.2.4.4.14 (±)(E) 4-Hydroxy-4-(4-hydroxyphenyl)-N-(p-tolyl)but-2-enamide (7n)

Brownish white (68%); mp 295–297 °C; $C_{17}H_{17}NO_3$; MW, 283.3; MS (ESI): *m/z*: found 283.43 [M^+], calc. 283.3; IR (ν, cm^{-1}): 3551.01, 3350.54, 1706.07, 1674.09; ^1H NMR (500 MHz, DMSO-d6) δ: 7.56 (d, *J* = 7.9 Hz, 2H), 7.17 (d, *J* = 8.7 Hz, 2H), 7.11 (t, *J* = 6.7 Hz, 1H), 6.79 (d, *J* = 6.5 Hz, 2H), 7.11 (d, *J* = 14.2 Hz, 2H), 7.22 (t, *J* = 13.1 Hz, 1H), 4.6 (d, *J* = 3.0 Hz, 1H), 10.3 (b, s, exch. D_2O, NH), 9.1 (b, s, OH), 5.3 (b, s, OH); ^{13}C NMR (125 MHz, DMSO-d6) δ: 167.3, 157.8, 143.2, 136.8, 134.7, 134.5, 129.8, 129.01, 123.1, 121.6, 116.1, 72.4, 21.6.

5.2.4.4.15 (±)(E) 4-Hydroxy-4(4-hydroxyphenyl)-N(4-nitrophenyl)but-2-enamide (7o)

Brown solid (67%); mp 302–304 °C; $C_{16}H_{14}N_2O_5$; MW, 314.3; MS (ESI): *m/z*: found 314.09 [M^+], calc. 314.3; IR (ν, cm^{-1}): 3551.01, 3350.54, 1706.07, 1674.09; ^1H NMR (500 MHz, DMSO-d6) δ: 7.8 (d, *J* = 7.9 Hz, 2H), 7.17 (d, *J* = 8.7 Hz, 2H), 7.71 (d, *J* = 6.5 Hz, 2H), 7.11 (d, *J* = 6.2 Hz, 2H), 7.22 (t, *J* = 13.2 Hz, 1H), 6.2 (d, *J* = 12.2 Hz, 1H), 4.76 (d, *J* = 3.6 Hz, 1H), 9.8 (b, s, exch. D_2O, NH), 9.1 (b, s, OH), 5.34 (b, s, OH); ^{13}C NMR (125 MHz, DMSO-d6) δ: 166.9, 157.7, 143.7, 143.4, 143.2, 134.4, 129.5, 124.1, 123.1, 119.9, 116.2, 71.5.

5.2.4.4.16 (±)(E) 4-Hydroxy-4(4-hydroxyphenyl)-N(quinolin-6-yl)but-2-enamide (7p)

Brown solid (68%); mp 320–324 °C; $C_{19}H_{16}N_2O_3$; MW, 320.4; MS (ESI): *m/z*: found 320.06 [M^+], calc. 320.4; IR (ν, cm^{-1}): 3551.01, 3350.54, 1706.07, 1674.09; ^1H NMR (500 MHz, DMSO-d6) δ: 8.53 (s, 1H), 7.61 (s, 1H), 7.87–756 (m, 4H), 7.11 (d, *J* = 8.7 Hz, 2H), 6.11 (d, *J* = 7.3 Hz, 2H), 7.28 (t, *J* = 12.6 Hz, 1H), 7.22 (d, *J* = 12.4 Hz, 1H), 4.26 (d, *J* = 2.6 Hz, 1H), 9.8 (b, s, exch. D_2O, NH), 9.08 (b, s, OH), 5.34 (b, s, OH); ^{13}C

NMR (125 MHz, DMSO-d6) δ: 167.1, 157.3, 145.2, 143.3, 141.5, 137.6, 134.2, 132.9, 132.4, 129.7, 129.6, 123.13, 121.9, 121.1, 120.6, 116.2, 72.3.

5.2.4.4.17 (±)(E) 4-Hydroxy-4(4-hydroxyphenyl)-N(quinolin-3-yl)but-2-enamide (7q)

Brown solid (68%); mp 323–325 °C; $C_{19}H_{16}N_2O_3$; MW, 320.4; MS (ESI): *m/z*: found 320.52 [M^{+2}], calc. 320.4; IR (ν, cm^{-1}): 3551.01, 3350.54, 1706.07, 1674.09; ^{1}H NMR (500 MHz, DMSO-d6) δ: 8.81 (s, 1H), 7.07 (s, 1H), 7.96–7.44 (m, 4H), 7.11 (d, *J* = 8.3 Hz, 2H), 6.72 (d, *J* = 7.5 Hz, 2H), 7.22 (t, *J* =12.6 Hz, 1H), 7.11 (t, *J* = 13.2 Hz, 1H), 4.06 (d, *J* = 3.6 Hz, 1H), 9.98 (b, s, exch. D_2O, NH), 9.09 (b, s, OH), 5.12 (b, s, OH); ^{13}C NMR (125 MHz, DMSO-d6) δ: 167.7, 157.4, 143.5, 143.3, 141.5, 137.6, 134.2, 129.7, 129.5, 129.1, 127.3, 126.1, 125.1, 124.8, 123.01, 116.2, 71.8.

5.2.4.4.18 (±)(E) 4-Hydroxy-4(4-hydroxyphenyl)-N(quinolin-8-yl)but-2-enamide (7r)

Brown solid (66%); mp 322–324 °C; $C_{19}H_{16}N_2O_3$; MW, 320.4; MS (ESI): *m/z*: found 320.09 [M^+], calc. 320.4; IR (ν, cm^{-1}): 3551.01, 3350.54, 1706.07, 1674.09; ^{1}H NMR (500 MHz, DMSO-d6) δ: 8.86 (d, *J* = 7.6 Hz, 1H), 8.43 (d, *J* = 8.7 Hz, 1H), 7.77– 7.56 (m, 4H), 7.11 (d, *J* = 7.5Hz, 2H), 6.73 (d, *J* = 7.2Hz, 2H), 7.24 (t, *J* = 12.7 Hz, 1H), 7.01 (d, *J* = 12.2 Hz, 1H), 4.06 (d, *J* = 3.6 Hz, 1H), 10.03 (b, s, exch. D_2O, NH), 9.07 (b, s, OH), 5.34 (b, s, OH); ^{13}C NMR (125 MHz, DMSO-d6) δ: 167.4, 157.4, 148.6, 143.3, 137.2, 136.7, 134.2, 133.8, 129.5, 129.2, 127.3, 121.2, 116.2, 123.0, 116.5, 113.8, 73.5.

5.2.4.4.19 (±)(E) 4-Hydroxy-4(4-hydroxyphenyl)-N(4-(trifluoromethyl)phenyl)but-2-enamide (7s)

Brownish yellow (71%); mp 302–304 °C; 308–310; MW, 337.3; MS (ESI): *m/z*: found 307.28 [M^+], calc. 337.3; IR (ν, cm^{-1}): 3551.01, 3350.54, 1706.07, 1674.09; ^{1}H NMR (500 MHz, DMSO-d6) δ: 7.57 (d, *J* = 7.6 Hz, 2H), 7.46 (d, *J* = 8.3 Hz, 2H), 7.11 (d, *J* = 7.5 Hz, 2H), 6.72 (d, *J* = 7.2 Hz, 2H), 7.23 (t, *J* = 12.7 Hz, 1H), 7.11 (d, *J* = 13.02 Hz, 1H), 4.16 (d, *J* = 2.6 Hz, 1H), 9.45 (b, s, exch. D_2O, NH), 9.03 (b, s, OH), 5.04 (b, s,

OH); ^{13}C NMR (125 MHz, DMSO-d6) δ: 167.1, 157.5, 143.3, 140.9, 134.3, 132.1, 129.5, 125.3, 124.2, 123.0, 121.9, 116.2, 73.5.

5.2.4.4.20 (±)(E) 4-Hydroxy-4(4-hydroxyphenyl)-N(4-methoxyphenyl)but-2-enamide (7t)

Yellow crystal (59%); mp 313–315 °C; $C_{17}H_{17}NO_4$; MW, 299.3; MS (ESI): *m/z*: found 299.26 [M^+], calc. 299.3; IR (ν, cm^{-1}): 3551.01, 3350.54, 1706.07, 1674.09; ^{1}H NMR (500 MHz, DMSO-d6) δ: 7.70 (d, *J* = 7.5 Hz, 2H), 7.11 (d, *J* = 7.7 Hz, 2H), 6.97 (d, *J* = 7.6 Hz, 2H), 6.72 (d, *J* = 7.6 Hz, 2H), 7.21 (t, *J* = 12.9 Hz, 1H), 6.19 (d, *J* = 12.4 Hz, 1H), 4.51 (d, *J* = 2.9 Hz, 1H), 3.86 (s, 3H), 9.8 (b, s, exch. D_2O, NH), 9.1 (b, s, OH), 4.34 (b, s, OH); ^{13}C NMR (125 MHz, DMSO-d6) δ: 169.91, 143.6, 141.5, 140.2, 128.8, 128.01, 127.6, 127.1, 123.2, 121.92, 73.5.

5.2.4.4.21 (±)(E) 4-Hydroxy-4(4-hydroxyphenyl)-N(3-(trifluoromethyl)phenyl)but-2-enamide (7u)

Brownish Yellow (56%); mp 302–304 °C; $C_{17}H_{14}F_3NO_3$; MW, 337.3; MS (ESI): *m/z*: found 337.23 [M^+], calc. 337.3; IR (ν, cm^{-1}): 3551.01, 3350.54, 1706.07, 1674.09; ^{1}H NMR (500 MHz, DMSO-d6) δ: 8.31 (s, 1H), 7.92 (d, *J* = 7.5 Hz, 1H), 7.61 (d, *J* = 7.7 Hz, 1H), 7.40 (t, *J* = 7.7 Hz, 1H), 7.11 (d, *J* = 7.5 Hz, 2H), 6.72 (d, *J* = 7.2 Hz, 2H), 7.28 (t, *J* = 12.8 Hz, 1H), 7.2 (t, *J* = 12.6 Hz, 1H), 4.36 (d, *J* = 2.6 Hz, 1H), 9.9 (b, s, exch. D_2O, NH), 9.03 (b, s, OH), 4.4 (b, s, OH); ^{13}C NMR (125 MHz, DMSO-d6) δ: 167.3, 157.4, 143.4, 139.6, 134.2, 131.2, 129.5, 129.2, 124.9, 124.1, 123.0, 120.7, 116.7, 116.1, 71.5.

5.2.4.4.22 (±)(E) N(4-Acetylphenyl)-4-hydroxy-4(4-hydroxyphenyl)but-2-enamide (7v)

Yellow brown (57%); mp 317–319 °C; $C_{18}H_{17}NO_4$; MW, 311.3; MS (ESI): *m/z*: found 311.08 [M^+], calc. 311.3; IR (ν, cm^{-1}): 3551.01, 3350.54, 1706.07, 1674.09;

^{1}H NMR (500 MHz, DMSO-d6) δ: 8.05 (d, *J* = 7.4 Hz, 2H), 7.76 (d, *J* = 7.7 Hz, 2H), 7.11 (d, *J* = 7.5 Hz, 2H), 6.72 (d, *J* = 7.4 Hz, 2H), 7.22 (t, *J* = 12.7 Hz, 1H), 7.1 (d, *J* = 12.5 Hz, 1H), 4.21 (d, *J* = 2.7 Hz, 1H), 2.53 (s, 3H), 10.13 (b, s, exch. D_2O, NH), 9.06 (b, s, OH), 5.04 (b, s, OH); ^{13}C NMR (125 MHz, DMSO-d6) δ: 169.91, 143.6, 141.5, 140.2, 128.8, 128.01, 127.6, 127.1, 123.2, 121.92, 73.5.

5.2.4.4.23 (±)(E) 4-Hydroxy-4(4-methoxyphenyl)-N(quinolin-8-yl)but-2-enamide (7w)

Brown crystal (57%); mp 327–329 °C; $C_{20}H_{18}N_2O_3$; MW, 334.4; MS (ESI): *m/z*: found 334.32 [M^+], calc. 334.4; IR (ν, cm^{-1}): 3551.01, 3350.54, 1706.07, 1674.09; ^{1}H NMR (500 MHz, DMSO-d6) δ: 8.86 (d, *J* = 7.1 Hz, 1H), 8.57 (d, *J* = 7.7 Hz, 1H), 7.77 (d, *J* = 7.3 Hz, 2H), 7.57–7.46 (m, 3H), 7.27 (d, *J* = 6.9 Hz, 2H), 6.89 (d, *J* = 7.7 Hz, 2H), 7.28 (t, *J* = 12.6 Hz, 1H), 7.2 (d, *J* = 12.5 Hz, 1H), 4.76 (d, *J* = 2.9 Hz, 1H), 3.82 (s, 3H), 10.13 (b, s, exch. D_2O, NH), 5.34 (b, s, OH); ^{13}C NMR (125 MHz, DMSO-d6) δ: 167.21, 159.5, 148.6, 143.3, 137.2, 136.7, 133.9, 133.7, 129.2, 129.0, 127.3, 123.1, 121.2, 116.5, 114.5, 113.8, 72.1, 55.8.

5.2.4.4.24 (±)(E) 4-Hydroxy-4(4-methoxyphenyl)-N(quinolin-6-yl)but-2-enamide (7x)

Brown solid (67%); mp 325–327 °C; $C_{20}H_{18}N_2O_3$; MW, 334.4; MS (ESI): *m/z*: found 334.09 [M^+], calc. 334.4; IR (ν, cm^{-1}): 3557.7, 3361.7, 1711.7, 1676.17; ^{1}H NMR (500 MHz, DMSO-d6) δ: 8.71 (d, *J* = 7.5 Hz, 1H), 8.53 (d, *J* = 7.1 Hz, 1H), 8.35 (d, *J* = 7.3 Hz, 1H), 7.46 (d, *J* = 6.9 Hz, 1H), 7.35 (t, *J* = 6.8 Hz, 1H), 7.28 (d, *J* = 7.2 Hz, 2H), 6.75 (s, 1H), 6.89 (d, *J* = 7.3 Hz, 1H), 7.28 (t, *J* = 12.7 Hz, 1H), 7.2 (t, *J* = 12.4 Hz, 1H), 4.96 (d, *J* = 2.6 Hz, 1H), 3.82 (s, 3H), 10.03 (b, s, exch. D_2O, NH), 5.34 (b, s, OH); ^{13}C NMR (125 MHz, DMSO-d6) δ: 167.4, 159.5, 145.2, 143.3, 141.5, 137.6, 133.9, 132.9, 132.4, 129.7, 129.2, 123.1, 121.9, 121.1, 120.6, 114.5, 72.2, 55.8.

5.2.5 Biological assays

5.2.5.1 *In vitro* cholinesterase inhibition

The AChE and BuChE inhibition studies were performed by modified Ellman *et al.* method [16] and the details have been described in Chapter 2, Section 2.2.17.

5.2.5.2 *In vitro* monoamine oxidase inhibition

5.2.5.2.1 Collection of MAO isoforms from rat brain mitochondria

Authorization for animal studies was obtained from the Central Animal Ethical Committee, Institute of Medical Sciences, Banaras Hindu University (Protocol No. Dean/13e14/CAEC/342). Albino Wistar rats (weight 200–220 g) were collected from Central Animal House, Institute of Medical Sciences, Banaras Hindu University. Mitochondria from rat brain (without cerebellum) were isolated with a slightly modified method of Berman S.B. *et al.* at 4 °C [17]. The brain was homogenized in the isolation buffer and centrifuged at 1300g for 5 min. Isolation buffer consisted a mixture of 215 mM mannitol, 75 mM sucrose, 0.1% w/v bovine serum albumin, 20 mM HEPES buffer and 1 mM of EGTA in 100 ml of deionized water and pH adjusted to 7.2 with KOH. The pellet was re-suspended in the isolation buffer and centrifuged, as mentioned earlier. The two supernatants were mixed and centrifuged at 14,000g for 10 min to obtain mitochondrial pellets. Pellets were rinsed with isolation buffer without EGTA and centrifuged at 14,000g for 10 min to take out EGTA. Mitochondrial protein was extracted out from pellets in PBS buffer by repeated centrifugation at 14,000g for 10 min, and the supernatant was collected. Total protein was estimated by Lowry O.H *et al.* absorptiometric method [18] and stored at −80 °C.

5.2.5.2.2 MAO inhibition assay

The inhibitory potency of the synthesized compounds on MAO activity was investigated by measuring their effect on the production of hydrogen peroxide from p-

tyramine (a common substrate for both MAO-A and MAO-B), benzylamine (a typical MAO-B substrates), 5-hydroxytryptamine (a typical MAO-A substrate) using the Amplex Red MAO assay kit (Thermo Fisher Scientific, USA). The MAO isoforms catalyzed H_2O_2 production and detected using 10-acetyl-3, 7-dihydroxyphenoxazine (Amplex Red reagent), a nonfluorescent, highly sensitive, and stable probe that reacted with H_2O_2 in the presence of horseradish peroxidase to produce a fluorescent product, resorufin [19]. Appropriate amounts of the rat MAO-A or MAO-B were adjusted to achieve the experimental conditions at same reaction velocity, *i.e.*, to oxidize (control) the same concentration of substrate: 165 pmol of *p*-tyramine/min (MAO-A, 1.1 μg; specific activity, 150 nmol of *p*-tyramine oxidized to *p* hydroxyphenyl acetaldehyde/min)/mg protein; MAO-B, 7.5 μg; specific activity, 22 nmol of p-tyramine transformed/min)/mg protein) [20].

Finally, 50 μL of sodium phosphate buffer (0.05 M, pH 7.4) containing various concentrations of the test compounds, reference inhibitors, and 150 μg protein with MAO isoforms was incubated for 15 min at 37 °C in a black 96-well microplate placed in the dark chamber. After the incubation, the reaction was started by adding (final concentrations) 200 μM Amplex Red reagent, 1 U/mL horseradish peroxidase, and 1 mM *p*-tyramine for MAO-A and benzylamine for MAO-B assay. The production of H_2O_2 and subsequently, of resorufin was estimated at 37°C in a multidetection microplate reader (Synergy H1 microplate reader (BioTek, USA) based on the fluorescence generated (excitation, 545 nm; emission, 590 nm) over a 15 min period. Simultaneously, control experiments were carried out by replacing the test compounds (synthesized compounds and inhibitors) with proper dilutions of the vehicles. Also, the possibility of the above test drugs to modify the fluorescence generated in the reaction mixture due to nonenzymatic inhibition (*e.g.*, for directly reacting with Amplex Red

reagent) was determined by adding these drugs to solutions containing only the Amplex Red reagent in a sodium phosphate buffer.

5.2.5.3 *In vitro* MMP-9 enzyme inhibition

Human MMP-9 inhibition of selected synthesized quinoline (as zinc-binding motif) derivatives was performed by utilizing human MMP-9 fluorometric drug discovery kit, RED and the method is described in Chapter 2, Section 2.2.16.

5.2.5.4 *In vitro* blood-brain barrier permeation assay

The possible *in vitro* blood-brain barrier (BBB) permeation of compounds was evaluated by parallel artificial membrane permeation assay (PAMPA) of BBB as described by Di L. *et al.* [21] and the details have been described in Chapter 2, Section 2.2.19.

5.2.5.5 Determination of cell viability and neuroprotection

MTT (3-(4, 5-dimethyl thiazol-2-yl)-2,5-diphenyltetrazolium bromide) assay [22] was performed to determine cytotoxicity of the representative synthesized compounds. Neuroprotectivity of selected compounds was determined by evaluating their ability to protect SH-SY5Y cells against L-glutamate excitotoxicity-induced apoptosis. The details of the method have been depicted in Chapter 2, Section 2.2.20.

5.2.6 Molecular dynamics simulation

Molecular dynamics simulations of compound **6m**-AChE, compounds **6n**-MAO-B, compounds **7k**-MAO-B and compound **7p**-MMP-9 complexes (Glide XP docked) were performed by utilizing Desmond package with the OPLS 2005 force field to model all peptide interactions [23, 24]. The method, described in Chapter 2, Section 2.2.21, was utilized.

5.3 Results and Discussion

5.3.1 Fragment-based drug design

Fragment-based drug design afforded some important fragments and their combination provided 4-oxo-N, 4-diphenylbutanamide as AChE as well as MAO-B inhibitor. The Glide XP docking scores of fragments with interactions with amino acid residue of AChE and MAO-B are shown in **Figures 5.3** and **5.4** respectively.

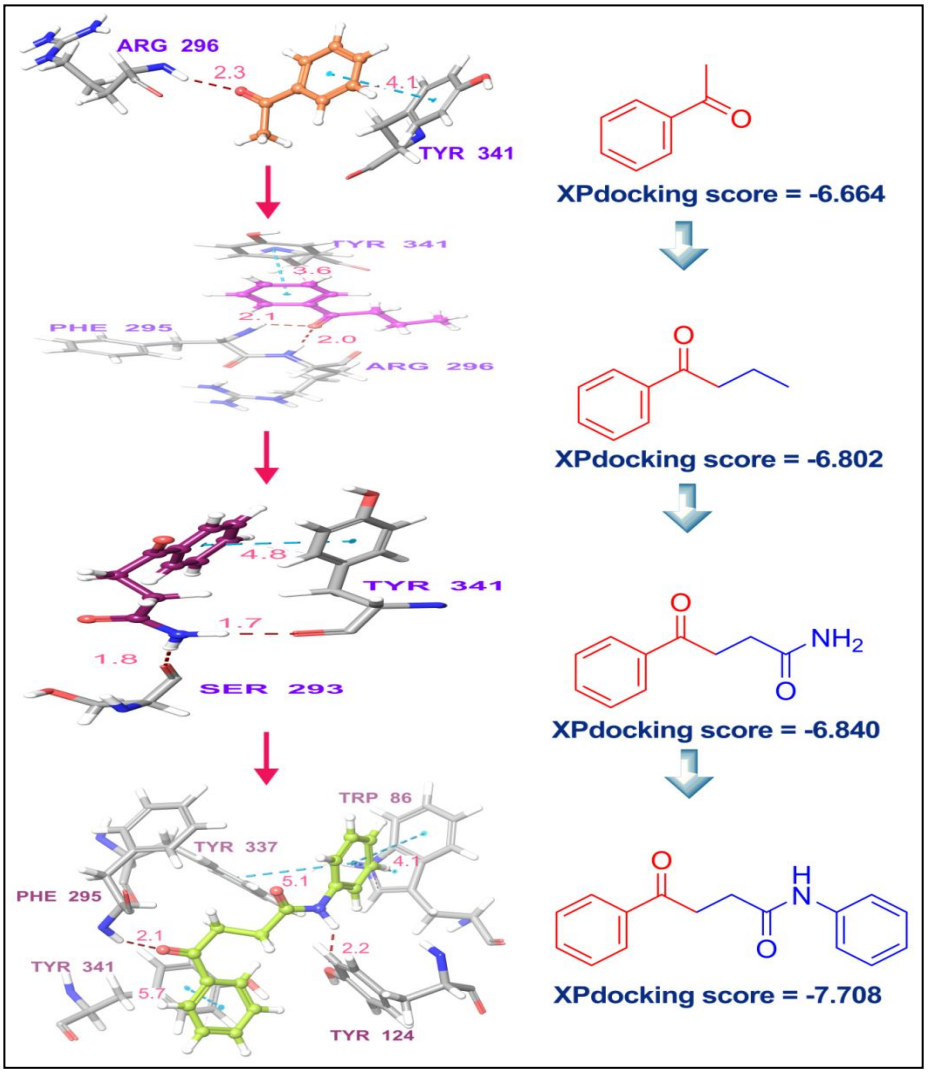

Figure 5.3 Docking poses and XP docking scores of fragments with interaction of amino acid residues of AChE.

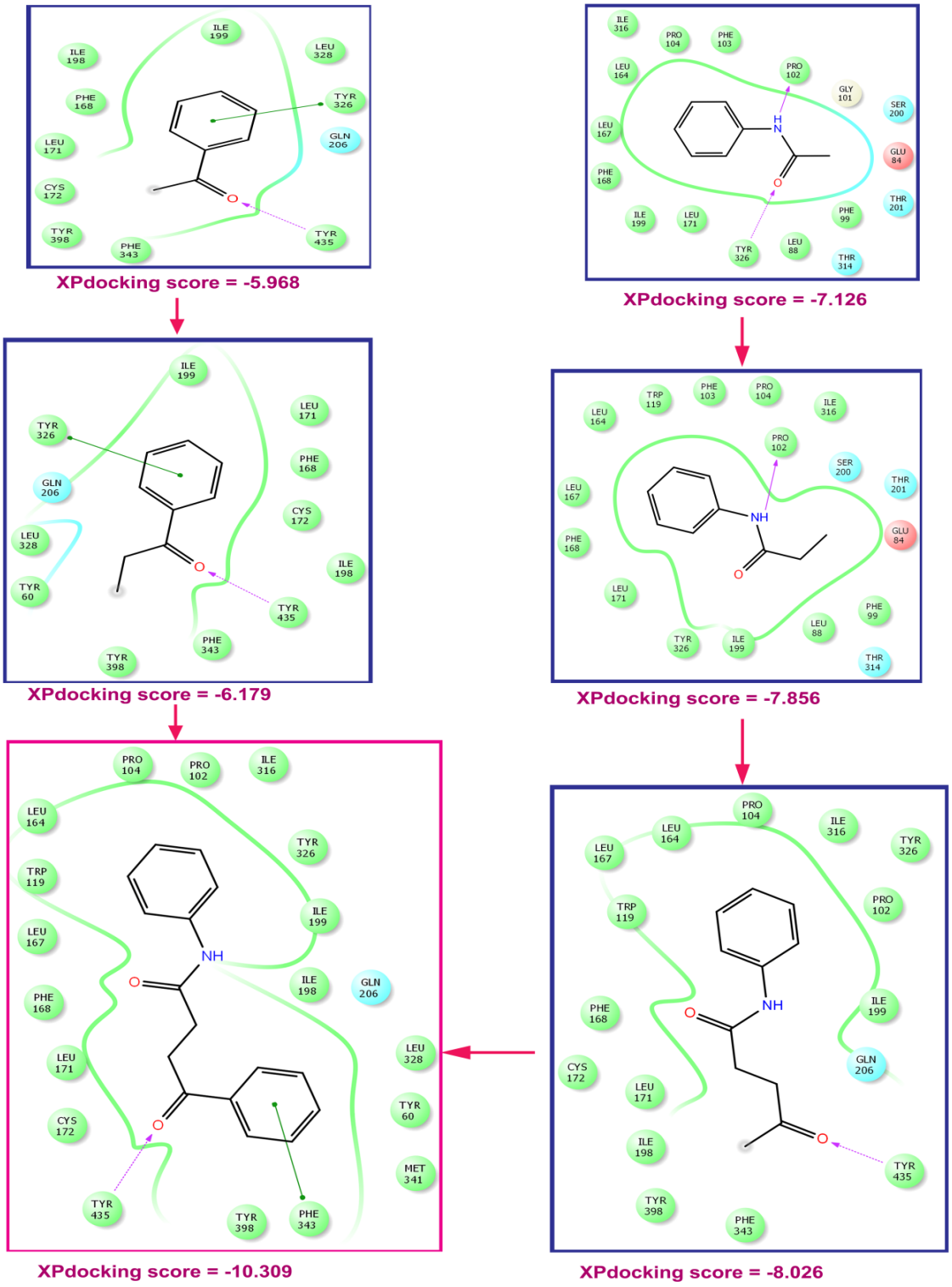

Figure 5.4 Docking poses and XP docking scores of fragments with interaction of amino acid residues of MAO-B

The selection of fragment was achieved on the basis of docking results and also impotent motif *i.e.*, N-ethylbenzamide, N-ethylpicolinamide, phenylamino and

benzylamino from moclobemide (MAO inhibitor), mazabemide (MAO inhibitor), edrophonium (AChE inhibitor), and donepezil (AChE inhibitor) respectively (**Figure 5.5**). Finally, 4-oxo-N, 4-diphenylbutanamide was established as hit after molecular docking and physiochemical descriptors calculation. 4-Oxo-N, 4-diphenylbutanamide, as cholinesterase and MAO inhibitor, encouraged to design (±) (E)-N-aryl-4-hydroxy-4-phenylbut-2-enamides, by modification at '4-oxo-butane' motif by '4-hydroxy but-2-ene'.

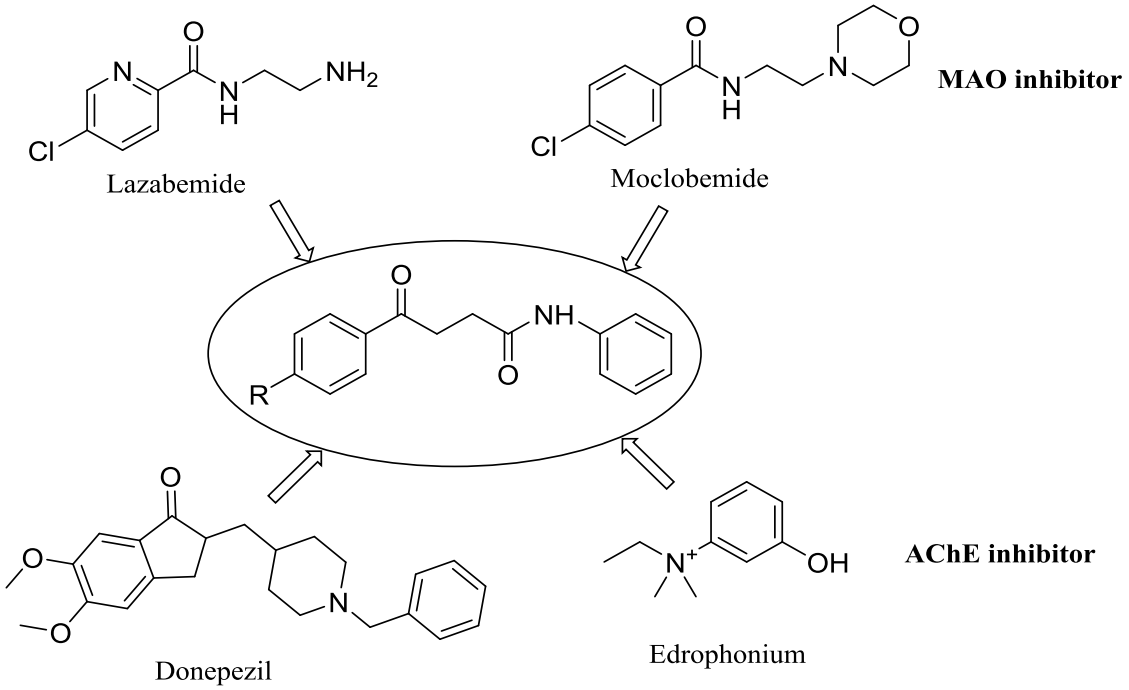

Figure 5.5 Rationale for designed molecules.

5.3.2 Molecular docking

Glide XP docking studies of 4-oxo-N, 4-diphenylbutanamides (**6a**–**6s**) and (±) (E)-N-aryl-4-hydroxy-4-phenylbut-2-enamides (**7a**–**7x**) were performed using Glide, Maestro against crystal structures of AChE, MAO-A, and MAO-B. Based on Glide docking score, Glide energy, and residue interactions, compounds were selected for further studies (**Tables 5.1**, and **5.2)**.

Table 5.1 Docking results of 4-oxo-N, 4-diphenylbutanamides against AChE, MAO-A, and MAO-B

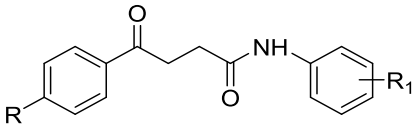

Compound	R	R_1	Docking score with AChE (4M0E)	Docking score with MAO-B (4A7A)	Docking Score with MAO-A (2Z5Y)
6a	H	H	−7.708	−10.111	−4.717
6b	H	4-Cl	−8.364	−10.482	−4.542
6c	H	3-Cl	−9.025	−10.541	−6.72
6d	H	4-Me	−7.754	−9.952	−4.237
6e	H	4-OMe	−8.823	−9.497	−6.598
6f	H	3-OMe	−8.249	−10.92	−4.675
6g	H	4-CF_3	−7.847	−10.966	−4.562
6h	H	3-CF_3	−7.455	−11.625	−7.573
6i	H	4-CN	−8.363	−9.584	−4.306
6j	H	3-CN	−7.955	−10.591	−4.006
6k	H	3-COMe	−8.479	−11.069	−7.534
6l	H	3-Me	−8.712	−10.271	−7.974
6m	H	4-COMe	−8.108	−11.237	−4.253
6n	H	4-OH	−8.76	−8.971	−7.131
6o	H	2-OMe, 4-NO_2	−9.058	−9.892	−6.833
6p	OH	4-COMe	−8.636	−10.535	−10.625
6q	Cl	4-COMe	−9.521	−11.158	−9.236
6r	Me	4-Cl	−8.447	−10.951	−6.985
6s	Me	3-F	−9.731	−9.261	−5.087
Donepezil	--	--	−8.236	---	----
Clorgyline	--	--	---	---	−6.798
Pargyline	--	--	---	−5.745	---

Table 5.2 Docking results of (±) (E)-N-aryl-4-hydroxy-4-phenylbut-2-enamides against AChE, MAO-A, and MAO-B

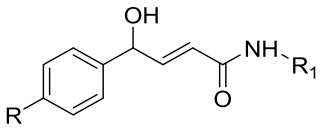

Comp	R	R_1	Docking score with 4M0E (AChE)		Docking score with 4A7A (MAO-B)		Docking score with 4Z5Y (MAO-A)	
			(S)	(R)	(S)	(R)	(S)	(R)
7a	H	Ph	−8.19	−8.02	−10.74	−10.54	−9.0	−9.08
7b	H	3-ClPh	−8.67	−8.83	−10.36	−10.81	−9.64	−9.43
7c	H	4-MePh	−7.94	−7.45	−10.54	−11.05	−9.10	−9.26
7d	H	4-OMePh	−8.42	−7.89	−10.02	−9.24	−8.31	−7.46
7e	H	3-CF_3Ph	−8.74	−8.05	−11.87	−11.58	−10.0	−10.03
7f	H	4-CNPh	−8.17	−7.83	−10.07	−11.07	−9.05	−9.0
7g	H	3-COMePh	−7.81	−9.84	−11.37	−7.21	−7.78	−9.47
7h	H	3,5-MePh	−8.0	−8.62	−10.16	−10.70	−8.98	−7.29
7i	H	4-COMePh	−8.68	−7.95	−11.6	−11.24	−10.5	−9.70
7j	H	2-OMe, 4-NO_2Ph	−6.65	−7.03	−8.59	−9.95	−7.70	−8.59
7k	Me	4-OHPh	−7.31	−9.11	−8.51	−9.00	−6.67	−9.11
7l	Cl	4-COMePh	−8.44	−8.29	−10.97	−8.52	−9.00	−9.12
7m	OH	4-ClPh	−8.32	−8.94	−10.29	−10.79	−9.38	−8.87
7n	OH	4-MePh	−8.25	−7.81	−10.47	−9.15	−8.46	−9.21
7o	OH	4-NO_2Ph	−9.03	−8.56	−8.83	−9.45	−7.90	−8.66
7p	OH	6-Quinolinyl	−11.04	−10.97	−11.4	−9.92	−10.4	−10.15
7q	OH	3-Quinolinyl	−9.44	−9.74	−11.61	−11.33	−9.88	−9.89
7r	OH	8-Quinolinyl	−9.94	−9.56	−10.94	−7.79	−9.83	−10.23
7s	OH	4-CF_3Ph	−8.25	−9.49	−11.64	−11.61	−8.68	−9.42
7t	OH	4-OMePh	−8.23	−7.93	−9.64	−9.48	−8.69	−8.79
7u	OH	3-CF_3Ph	−10.28	−8.96	−10.06	−11.65	−10.4	−10.69
7v	OH	4-COMePh	−9.73	−9.04	−9.62	−10.48	−9.79	−9.85
7w	OMe	8-Quinolinyl	−9.15	−9.74	−10.96	−8.89	−9.27	−9.32
7x	OMe	6-Quinolinyl	−9.64	−8.97	−8.11	−10.91	−9.85	−9.6

All the molecules having better Glide XP docking results than the reference compounds were picked up for further studies. In general (±) (E)-N-aryl-4-hydroxy-4-phenylbut-2-enamides (**7a**–**7x**) showed better docking scores than 4-oxo-N, 4-diphenylbutanamides (**6a**–6**s**) as cholinesterase and MAO inhibitors, due to some rigidity of 'but-2-ene' than 'butane'.

Compound **6s** showed better docking score with AChE (−9.731 kcal mol^{-1}) and MAO-B (−9.261 kcal mol^{-1}) crystal structures, while less binding affinity with MAO-A (−5.087 kcal mol^{-1}). Compound **6h** provided best docking score with MAO-B (−11.625 kcal mol^{-1}) and with MAO-A (−7.573 kcal mol^{-1}). Compound **6p** afforded best binding affinity with MAO-A (−10.625 kcal mol^{-1}). Compound **7p** showed better AChE binding affinity for both isomers (−11.04 kcal $mol^{-1}$and −10.97 kcal mol^{-1}), whereas, compound **7e** (−11.87 kcal $mol^{-1}$and −11.58 kcal mol^{-1}), **7i** (−11.6 kcal mol^{-1} and −11.24 kcal mol^{-1}), **7q** (−11.61 kcal mol^{-1} and −11.33 kcal mol^{-1}), and **7s** (−11.64 kcal mol^{-1} and −11.61 kcal mol^{-1}) provided better binding affinity towards MAO-B. All the designed molecules showed good MAO-B selective binding properties with moderate AChE binding interaction in comparison to reference compounds.

5.3.3 Determination of drug-likeness

Physiochemical descriptors of 4-oxo-N, 4-diphenylbutanamides (**6a**–**6s**) and (±) (E)-N-aryl-4-hydroxy-4-phenylbut-2-enamides (**7a**–**7x**) were calculated by using QikProp, Maestro. All the designed molecules showed acceptably predicted drug-like properties (**Tables 5.3** and **5.4**). These properties along with docking results, were considered for of final selection ligands for synthesis in both the series. Compounds **6a**–**6s** provided acceptable drug-likeness properties, *i.e.,* partition coefficient, QPlog Po/w for octanol/water (1.729–3.901); predicted aqueous solubility, QPlog S, in mol dm^{-3} (−5.06 to −3.43); log HERG, HERG K^+ channel blockage (−6.102 to −5.573); apparent Caco-2

cell permeability (165.902 – 1796.547 nm/s); QPlogBB, brain/blood partition coefficient (−0.245 to −1.755); apparent MDCK permeability (70.975 to 3907.338 nm/s); QPlogKp: skin permeability (−3.34 to −1.16); % Human oral absorption (76.79 – 100).

Table 5.3 Calculated physiochemical descriptors of 4-oxo-N, 4-diphenylbutanamides using QikProp

Comp	QPlog Po/w[a]	QPlog S[b]	QPlog HERG[c]	QPP Caco[d]	QPlog BB[e]	QPPM DCK[f]	QPlog Kp[g]	% Oral absorption[h]
6a	3.052	−4.18	−5.974	1722.72	−0.496	890.6	−1.16	100.0
6b	3.348	−4.64	−5.906	1722.91	−0.338	2199.1	−1.32	100.0
6c	3.39	−4.50	−5.906	1723.08	−0.339	2195.2	−1.32	100.0
6d	3.222	−4.47	−5.911	1722.86	−0.519	890.7	−1.35	100.0
6e	3.019	−3.87	−5.896	1718.57	−0.579	888.3	−1.26	100.0
6f	3.046	−3.84	−5.869	1796.55	−0.555	931.9	−1.21	100.0
6g	3.894	−5.02	−5.963	1719.15	−0.246	3878.6	−1.39	100.0
6h	3.901	−5.06	−5.976	1723.65	−0.245	3907.4	−1.39	100.0
6i	2.173	−4.62	−6.102	356.93	−1.303	162.5	−2.51	85.35
6j	2.173	−4.62	−6.102	357.89	−1.301	162.9	−2.51	85.38
6k	2.425	−3.84	−5.975	579.941	−1.09	274.5	−2.22	90.60
6l	3.467	−4.77	−5.84	1722.83	−0.543	890.6	−1.55	100.0
6m	2.456	−3.89	−6.011	547.867	−1.125	258.2	−2.28	90.35
6n	2.208	−3.43	−5.853	521.965	−1.089	245.0	−2.22	88.51
6o	2.313	−3.69	−5.573	234.557	−1.501	103.2	−3.01	82.91
6p	1.729	−3.76	−5.887	165.902	−1.755	70.97	−3.34	76.79
6q	2.899	−4.62	−5.928	549.265	−0.977	639.3	−2.44	92.96
6r	3.721	−4.94	−5.839	1721.76	−0.362	2197.5	−1.52	100.0
6s	3.464	−4.61	−5.795	1722.05	−0.412	1610.9	−1.49	100.0

[a]QPlog Po/w for octanol/water (−2.0 to 6.5); [b]QPlog S: Predicted aqueous solubility, S in mol dm^{-3} (−6.5 to 0.5); [c]log HERG: HERG K^+ channel blockage (<−5); [d]Apparent Caco-2 cell permeability (nm/s) (<25 poor, >500 great); [e]Apparent MDCK permeability (nm/s) (<25 poor, >500 great); [f]QPlogBB: brain/blood partition coefficient (–3.0 to 1.2); [g]QPlogKp: skin permeability (–8.0 to –1.0);[h]% Human oral absorption (>80% is high and <25% is poor).

Table 5.4 Calculated physiochemical properties of (E)-N-aryl-4-hydroxy-4-phenylbut-2-enamides using QikProp

Comp	QPlog Po/w[a]	QPlog S[b]	QPlog HERG[c]	QPP Caco[d]	QPlogBB[e]	QPPMDCK[f]	QPlog Kp[g]	% Oral absorbance[h]
7a	2.94	−3.95	−6.41	1355.86	−0.64	687.48	−1.25	100.0
7b	3.37	−4.72	−6.38	1162.10	−0.56	1434.06	−1.54	100.0
7c	3.22	−4.49	−6.32	1355.47	−0.66	687.27	−1.44	100.0
7d	3.04	−4.21	−6.31	1354.85	−0.72	686.92	−1.35	100.0
7e	3.86	−5.39	−6.42	1176.27	−0.46	2568.73	−1.59	100.0
7f	2.23	−5.01	−6.51	281.38	−1.47	125.63	−2.59	83.82
7g	2.47	−4.25	−6.37	457.46	−1.25	212.44	−2.31	89.03
7h	3.53	−5.06	−6.24	1355.51	−0.69	687.29	−1.64	100.0
7i	2.61	−4.30	−6.41	431.09	−1.29	199.23	−2.36	89.36
7j	2.38	−4.17	−6.05	192.38	−1.68	83.3	−3.07	81.75
7k	2.47	−4.19	−6.19	410.86	−1.29	189.15	−2.50	88.16
7l	2.94	−5.01	−6.31	431.06	−1.15	491.82	−2.53	91.31
7m	2.65	−4.37	−6.19	410.66	−1.11	466.76	−2.47	89.26
7n	2.47	−4.19	−6.19	410.59	−1.29	189.01	−2.50	88.16
7o	1.51	−3.90	−6.21	49.08	−2.36	19.03	−4.21	66.04
7p	2.46	−4.48	−6.78	254.62	−1.55	112.77	−2.56	84.44
7q	2.47	−4.48	−6.78	254.45	−1.55	112.69	−2.56	84.44
7r	2.54	−4.39	−6.75	334.42	−1.4	151.42	−2.29	87.0
7s	3.12	−5.01	−6.22	410.52	−1.03	824.17	−2.54	91.98
7t	2.29	−3.94	−6.18	410.35	−1.35	188.9	−2.41	87.13
7u	3.13	−5.02	−6.24	415.68	−1.02	834.5	−2.53	92.15
7v	1.73	−4.07	−6.28	130.56	−1.94	54.78	−3.43	74.95
7w	3.39	−4.99	−6.77	1103.16	−0.85	550.09	−1.34	100.0
7x	3.31	−5.0	−6.8	840.27	−0.99	409.88	−1.60	100.0

[a]QPlog Po/w for octanol/water (−2.0 to 6.5); [b]QPlog S: Predicted aqueous solubility, S in mol dm^{-3} (−6.5 to 0.5); [c]log HERG: HERG K^+ channel blockage (<−5); [d]Apparent Caco-2 cell permeability (nm/s) (<25 poor, >500 great); [e]Apparent MDCK permeability (nm/s) (<25 poor, >500 great); [f]QPlogBB: brain/blood partition coefficient (–3.0 to 1.2); [g]QPlogKp: skin permeability (–8.0 to –1.0);[h]% Human oral absorption (>80% is high and <25% is poor).

The other series of compounds (**7a**–**7x**) also showed well *in silico* drug-likeness properties, *i.e.*, partition coefficient, QPlog Po/w for octanol/water (1.51–3.86); predicted aqueous solubility, QPlog S, in mol dm^{-3} (−5.39 to −3.94); HERG K^+ channel blockage (−6.8 to −6.05); apparent Caco-2 cell permeability (nm/s) (49.08 – 1355.86); brain/blood partition coefficient (−2.36 to −0.46); apparent MDCK permeability (nm/s) (29.03 – 2568.73); skin permeability (−4.21 to −1.25); and % human oral absorption (74.95 – 100). Hence, these compounds are predicted to be weak inhibitors of HERG.

5.3.4 Organic synthesis

All the designed compounds were synthesized (procedure described in Section 5.2.4) and characterized by conventional spectral analysis, and determination of melting point, and solubility. The purity of the compounds was determined by HPLC (Appendix; **Table A.5**) and found to be above 98%. The HPLC chromatograms of compounds **6h** and **7h,** detected at 250 nm, are depicted in **Figures 5.6** and **5.7** respectively.

5.3.5 Biological assays

5.3.5.1 *In vitro* cholinesterase inhibition

Cholinesterase (AChE and BuChE) inhibition activities of synthesized molecules were evaluated by the method described by Ellman [16], wherein donepezil was used as the reference standard. The IC_{50} values of 4-oxo-N-4-diphenylbutanamides (**6a**–**s**) and (±)(E)-N-aryl-4-hydroxy-4-phenylbut-2-enamides (**7a**–**x**) were calculated by constructing a dose-response curve by utilizing GraphPad Prism 5.0 (**Tables 5.5** and **5.6** respectively). Compounds **6k** and **6p** contributed IC_{50} values against AChE within nanomolar range (0.877±0.21 and 0.691±0.43 nM respectively). In other series, compounds **7g**, **7k**, **7l**, **7o**, **7u** and **7v** also produced good IC_{50} values against AChE (0.942±0.32, 0.952±0.26, 0.756±0.26, 0.861±0.10, 0.734±0.20, 0.989±0.15 nM respectively).

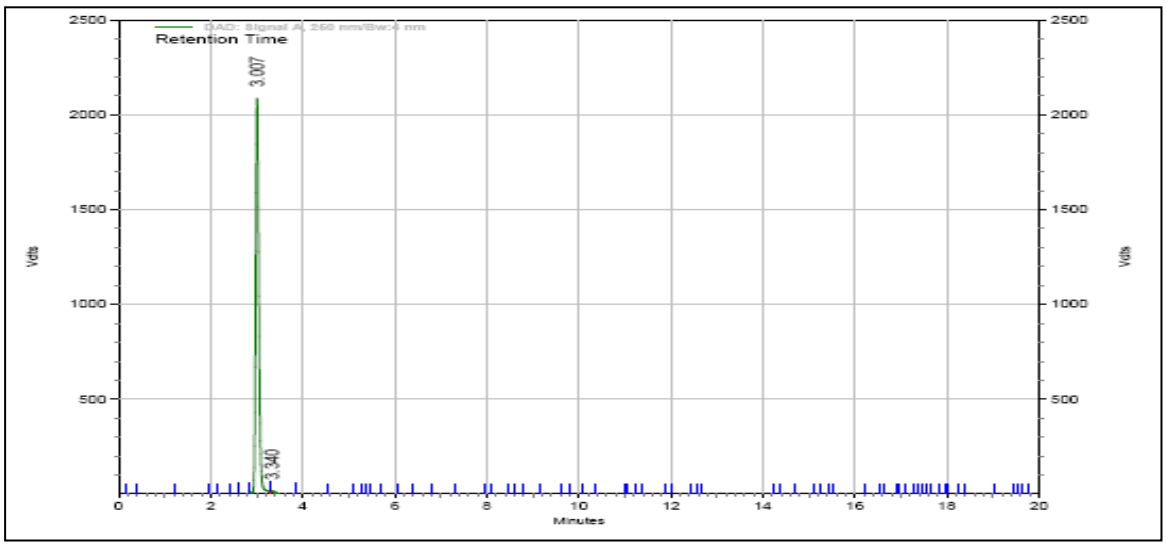

Figure 5.6 HPLC Chromatogram (t_R, 3.007 min) of compound **6h** at 250 nm.

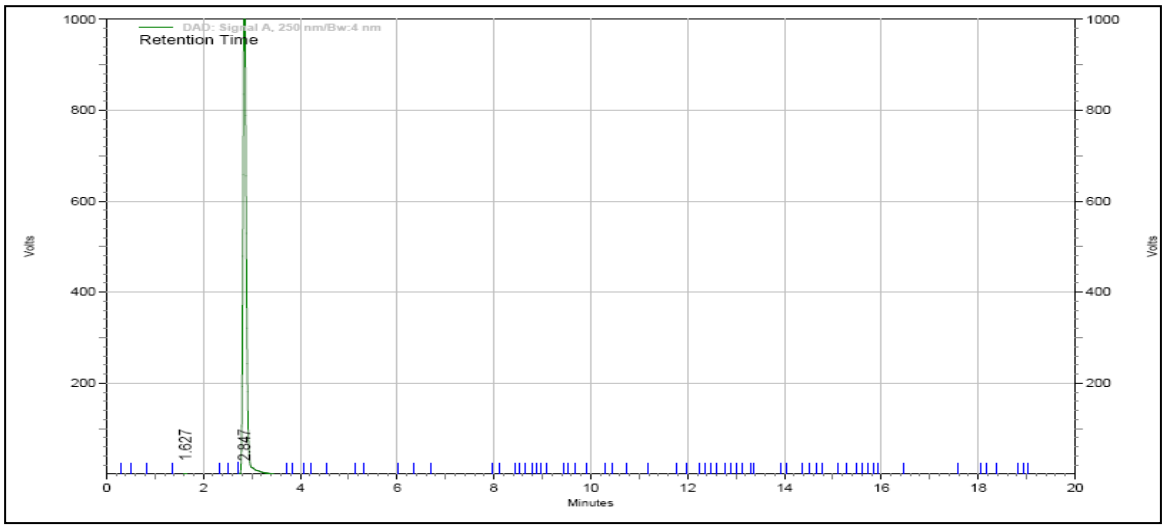

Figure 5.7 HPLC Chromatogram (t_R, 2.847 min) of compound **7h** at 250 nm.

5.3.5.2 *In vitro* monoamine oxidase inhibition

(±) (E)-N-Aryl-4-hydroxy-4-phenylbut-2-enamides (**7a**–**x**) showed potent MAO-**B** inhibition than 4-oxo-N, 4-diphenylbutanamides (**6a**–**s**). The IC_{50} values of all the synthesized molecules were calculated by constructing a dose-response curve by using GraphPad Prism 5.0 (**Tables 5.5** and **5.6**). Compounds **6m** (IC_{50}, 11.537±0.06 nM), **6h** (IC_{50}, 17.253±0.09 nM), **6i** (IC_{50}, 28.199±0.02 nM) and **6j** (IC_{50}, 15.853±0.016 nM) showed potent and selective MAO-B inhibition from 4-oxo-N, 4-diphenylbutanamide

series. However, compounds **6k**, **6n,** and **6p** contributed both MAO-B, MAO-A inhibitions, and compound **6q** showed selective MAO-A inhibition (IC_{50}, 47.289±0.08 nM).

Table 5.5 Inhibitory activity of 4-oxo-N, 4-diphenylbutanamides on AChE (*electric eel*), BChE (horse serum), MAO-A, and MAO-B

Compound	**AChE[a] IC_{50}(μM)**	**BuChE[a] IC_{50}(μM)**	**Selectivity[b]**	**MAO-A[a] IC_{50}(nM)**	**MAO-B[a] IC_{50}(nM)**	**Selectivity[c]**
6a	2.790±0.31	34.22±1.04	12.268	63.19±0.41	47.827±0.70	1.321
6b	1.909±0.17	184.74±1.13	96.775	85.13±0.30	20.895±0.50	4.074
6c	2.167±0.66	167.07±1.27	77.116	>1000	69.394±0.13	-
6d	3.136±0.84	146.39±1.29	46.681	>1000	53.855±0.18	-
6e	1.235±0.81	46.06±0.65	37.292	68.26±0.090	48.146±0.26	1.418
6f	2.721±0.15	164.05±1.24	60.298	145.04±0.13	34.836±0.31	4.163
6g	3.281±0.95	135.85±0.83	41.401	155.9±0.052	44.705±0.50	3.487
6h	3.622±0.11	168.75±2.07	46.585	198.93±0.60	17.253±0.90	11.530
6i	2.976±0.75	142.12±1.06	47.756	188.04±0.07	28.199±0.20	6.668
6j	3.165±0.9	82.67±0.88	26.116	136.1±0.24	15.853±0.16	8.585
6k	0.877±0.21	32.15±0.79	36.656	37.85±0.57	25.092±0.27	1.509
6l	1.201±0.85	22.59±0.74	18.814	50.2±0.31	30.528±0.42	1.644
6m	1.221±0.47	49.93±0.829	40.885	76.99±0.071	11.537±0.64	6.673
6n	1.511±0.83	37.56±1.27	24.864	22.84±0.17	16.813±0.85	1.358
6o	1.250±0.41	62.64±0.94	50.094	85.51±0.05	59.287±0.42	1.442
6p	0.691±0.43	58.75±1.25	85.044	37.21±0.40	25.194±0.17	1.477
6q	2.796±0.47	38.65±0.92	13.824	47.29±0.08	69.902±0.21	0.677
6r	2.071±0.59	332.04±2.36	160.359	219.99±0.32	46.903±0.83	4.690
6s	3.250±0.45	82.55±0.86	25.398	185.84±0.15	87.132±0.51	2.133
Chlorgyline	-	-	-	5.04±0.032	62.027±0.22	0.081
Pargyline	-	-	-	12.25±0.24	9.036±0.37	1.355
Donepezil	0.017±0.0011	6.16±0.015	360.356	-	-	-

[a]Each assay was repeated three times independently; [b]Selectivity for AChE=[IC_{50} (BuChE)]/[IC_{50} (AChE)], [c]Selectivity for MAO=[IC_{50}(MAO-A)]/[IC_{50}(MAO-B)]

Table 5.6 Inhibitory activity of (±)(E)-N-aryl-4-hydroxy-4-phenylbut-2-enamides on AChE , BChE, rat MAO-A, ratMAO-B and hMMP-9

Compound	AChE[a]*	BuChE[a]*	Selectivity[c]	MAO-A[b]*	MAO-B[b]*	Selectivity[d]	MMP-9[b]*
7a	1.04±0.34	35.58±1.58	34.368	56.97±0.21	50.02±0.32	1.139	-
7b	1.69±0.35	54.43±1.21	32.189	150.89±0.5	69.34±0.52	2.176	-
7c	1.15±0.12	53.29±1.27	46.165	48.41±0.14	34.43±0.21	1.406	-
7d	1.46±0.21	49.76±2.30	34.199	59.49±0.19	65.99±0.82	0.901	-
7e	2.7±0.8	40.62±2.19	15.057	185.57±0.7	82.36±0.25	2.253	-
7f	1.08±0.24	49.53±2.15	46.075	38.75±0.13	30.25±0.19	1.281	-
7g	0.94±0.32	50.74±2.33	53.840	45.75±0.16	15.70±0.83	2.913	-
7h	1.04±0.25	>200	480.46	71.35±0.51	34.63±0.32	2.060	-
7i	1.06±0.13	40.38±2.16	38.209	87.94±0.23	51.18±0.63	1.718	-
7j	1.06±0.12	41.77±2.23	39.516	46.02±0.13	44.96±0.17	1.024	-
7k	0.95±0.26	32.36±2.21	34.012	6.22±0.19	3.18±0.72	1.958	-
7l	0.76±0.26	38.65±1.48	51.138	52.63±0.73	50.35±0.21	1.045	-
7m	1.03±0.58	31.52±1.24	30.651	58.14±0.15	32.54±0.18	1.787	-
7n	1.36±0.46	30.41±1.13	22.415	50.37±0.16	28.81±0.14	1.748	-
7o	0.86±0.10	40.30±1.19	46.795	21.44±0.24	28.69±0.43	0.747	-
7p	1.53±0.11	20.78±1.21	13.629	28.74±0.53	6.953±0.72	4.131	167.2±0.7
7q	1.77±0.26	31.67±1.43	17.929	44.35±0.67	8.57±0.18	5.174	242.3±0.9
7r	1.85±0.31	22.13±1.27	11.953	47.89±0.37	10.04±0.23	4.768	173.9±0.5
7s	1.65±0.22	17.51±1.37	10.595	48.49±0.18	5.73±0.53	8.469	-
7t	1.55±0.29	29.41±1.39	19.155	33.04±0.26	11.84±0.32	2.789	-
7u	0.73±0.20	22.86±1.36	31.143	11.23±0.48	3.86±0.17	2.907	-
7v	0.99±0.15	31.41±1.39	31.756	23.66±0.74	5.27±0.27	4.490	-
7w	1.09±0.13	53.93±2.24	49.613	112.21±1.1	82.93±0.73	1.353	230.7±0.3
7x	1.34±0.28	71.53±2.57	53.249	52.07±0.49	50.83±0.43	1.024	-
Clorgiline	-	-	-	4.98±0.31	61.57±0.12	0.081	-
Pargyline	-	-	-	11.98±0.53	8.49±0.32	1.411	-
Donepezil	0.016±0.005	6.783±0.15	413.593	-	-	-	-
NNGH	-	-	-	-	-	-	3.107±0.8

[a]IC_{50} in µM; [b]IC_{50} in nM; *Each assay was repeated three times independently; [c]Selectivity for AChE=[IC_{50} (BuChE)]/[IC_{50} (AChE)]; [d]Selectivity for MAO=[IC_{50} (MAO-A)]/[IC_{50} (MAO-B)].

In other series, compounds **7k**, **5p**, **7s, 7u**, and **7v** provided more potent MAO-B inhibition (IC_{50} values, 3.178±0.02, 6.953±0.072, 5.726±0.053, 3.863±0.17, 5.270±0.13 nM respectively) than pargyline, and compound **7p** allowed similar IC_{50} value (8.572±0.018 nM) that of pargyline, whereas compounds **7d** and **7o** showed selective MAO-A inhibition (IC_{50}, 59.485±0.09 and 21.436±0.24 nM respectively).

5.3.5.3 *In vitro* MMP-9 enzyme inhibition

The (±)(E)-N-quinolinyl-4-hydroxy-4-phenylbut-2-enamides showed MMP-9 inhibition due to presence of quinolinyl as 'zinc binding group' (**Table 5.6**). Compound **7p** provided potent MMP-9 inhibitor (IC_{50}, 167.2±0.074 nM) than other compounds **7q**, **7r**, and **7w** (IC_{50}, 242.3±0.093, 173.9±0.053 and 230.7±0.032 respectively) along with selective MAO-B inhibition. MMP-9 inhibition was diminished by the conversion of 4-OH group (compound **7p**) to 4-OMe (compound **7w**) at 4-phenyl ring.

5.3.5.4 *In vitro* blood-brain barrier permeation assay

PAMPA of blood-brain barrier was performed to investigate permeation of synthesized compounds into the brain. It was performed by the technique described by Di L. *et al.* [21]. The *in vitro* permeability (Pe) of nine commercially available drugs (**Table 5.7**) was determined over a lipid extract of porcine brain lipid in PBS. The assay was endorsed by comparing the experimentally obtained permeability [Pe(exp)] of the nine drugs with literature values of permeation [Pe(ref)] offering a linear relationship (**Figure 5.8**), *i.e.*, $Pe(exp) = 1.316Pe(literature) - 0.9281$, ($R^2 = 0.987$).

The permeability values, Pe (exp) greater than 4.28×10^{-6} cm s^{-1}, was considered as high BBB permeable molecule, Pe (exp) less than 1.65×10^{-6} cm s^{-1}, compound recognized as low BBB permeable, and Pe (exp) within these values, as medium BBB permeable. The *in vitro* permeability (Pe) of synthesized molecules (**Tables 5.8** and **5.9**) were determined. The compound with permeability values greater than 4.28×10^{-6} cm

s^{-1} were able to penetrate CNS (**Tabless 5.7**, and **5.8**) and most of synthesized compounds (except compounds **6n**, **6o**, **6q**, and **7q** showed less BBB permeability) denoted permeability values above it. Thus, the synthesized compounds were expected to cross the BBB by passive diffusion comfortably.

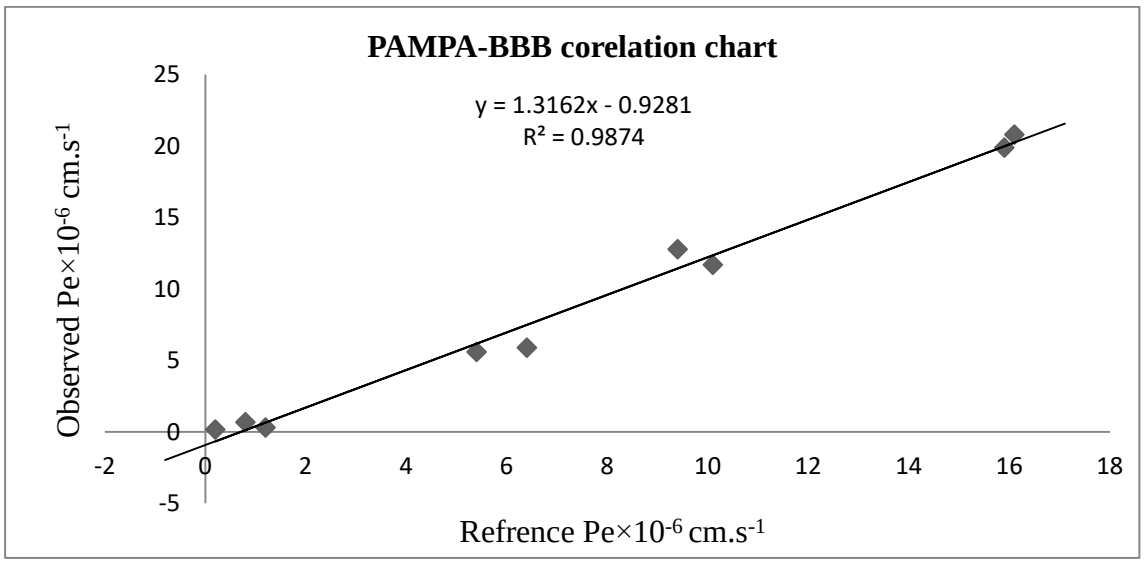

Figure 5.8 Linear correlation chart of experimental and literature reported permeability of commercial drugs for PAMPA-BBB assay.

Table 5.7 Permeability of nine commercial drugs used for validation of PAMPA-BBB assay

Commercial drug	**Reference value Pe (10^{-6})*[a]**	**Experimental value Pe (10^{-6})*[b]**
Verapamil	16.1	20.81±1.2
Diazepam	15.9	19.9±0.5
Progesterone	9.4	12.79±1.12
Atenolol	0.8	0.68±0.4
Dopamine	0.2	0.17±0.1
Lomefloxacin	1.2	0.31±0.3
Alprazolam	5.4	5.6±0.7
Chlorpromazine	6.4	5.9±0.6
Oxazepam	10.1	11.7±1.1

[a]Taken from literature; [b]Data are expressed as mean ± SEM of three independent experiments; *Permeability (Pe 10^{-6}) express in cm s^{-1}.

Table 5.8 Permeability of 4-oxo-N, 4-diphenylbutanamides determined by BBB-PAMPA assay

Compound	Pe[10^{-6}cm s^{-1}]*[a]	Prediction[b]
6a	5.30±0.16	CNS+
6b	11.17±0.38	CNS+
6c	19.01±0.6	CNS+
6d	6.43±0.57	CNS+
6e	7.78±0.51	CNS+
6f	19.54±0.23	CNS+
6g	5.36±0.32	CNS+
6h	5.95±0.19	CNS+
6i	13.60±0.38	CNS+
6j	10.73±0.21	CNS+
6k	13.64±0.15	CNS+
6l	16.65±0.4	CNS+
6m	9.63±0.23	CNS+
6n	1.44±0.39	CNS−
6o	0.55±0.50	CNS−
6p	11.35±0.28	CNS+
6q	1.24±0.47	CNS−
6r	9.94±0.37	CNS+
6s	9.24±0.53	CNS+

[a]Data expressed as mean± SEM of three independent experiments; [b]CNS+ indicates good, and CNS− indicates poor passive CNS permeation, *Permeability (Pe 10^{-6}) express in cm s^{-1}.

5.3.5.5 Structure-activity relationship studies

In vitro studies revealed that (±) (E)-N-aryl-4-hydroxy-4-phenylbut-2-enamides (**7a**–**x**) were more potent MAO-B inhibitors than 4-oxo-N, 4-diphenylbutanamides (**6a**–**s**) due to some rigidity of 2-butene moiety. Compounds 6a–s are freely rotatable and generate

number of conformations for each molecule. Introduction of double bond (**7a**–**x**) restrict the number of possible conformations generated and improves the chances of active conformation being locked within the active site, thus increasing the activity of compounds **7a**–**x**. *Para* substitution of COMe group (compound **6m**) afforded potent, selective MAO-B inhibitor, whereas the *meta* substitution of COMe (compound **6k**) reduced the selectivity as well as MAO-B inhibition potency. Halogen substitution (Cl and F) at 4-phenyl reduced the MAO-B activity, whereas 4-OH substitution at 4-phenyl (compound **6p**) or N-phenyl (compound **6n**) ring increased the MAO-B inhibition.

Table 5.9 Permeability of (±) (E)-N-aryl-4-hydroxy-4-phenylbut-2-enamides determined by BBB-PAMPA study

Compound	**Pe[10^{-6}cm s^{-1}]^{a*}**	**Prediction^{b}**	**Compound**	**Pe[10^{-6}cm s^{-1}]^{a*}**	**Prediction^{b}**
7a	4.22±0.14	CNS+	7m	9.43±0.09	CNS+
7b	23.30±0.39	CNS+	7n	2.97±0.3	CNS+
7c	8.19±0.084	CNS+	7o	4.19±0.21	CNS+
7d	4.93±0.027	CNS+	7p	3.77±0.4	CNS+
7e	13.51±0.18	CNS+	7q	0.84±0.36	CNS−
7f	7.82±0.26	CNS+	7r	2.38±0.05	CNS+
7g	4.24±0.09	CNS+	7s	1.87±0.73	CNS
7h	6.49±0.19	CNS+	7t	2.07±0.2	CNS+
7i	9.01±0.27	CNS+	7u	5.81±0.39	CNS+
7j	4.10±0.35	CNS+	7v	2.20±0.048	CNS
7k	4.19±0.14	CNS+	7w	1.97±0.4	CNS
7l	3.27±0.46	CNS+	7x	2.15±0.62	CNS+

[a]Data expressed as mean± SEM of three independent experiments; [b]CNS+ indicates good, CNS indicates medium, and CNS− indicates poor passive CNS permeation, *Permeability (Pe 10^{-6}) express in cm s^{-1}.

Further, substitution of 3-CF_3 (compound **6h**), and 3-CN (compound **6j**) at N-phenyl provided potent and selective MAO-B inhibitors whereas, *para*-substitutions (compounds **6g**, and **6i** respectively) reduced the activity. The 4-Cl group at N-phenyl ring (compound **6b**) increased the potency and selectivity of MAO-B than 3-Cl group (compound **6c**), but 4-Me group at 4-phenyl (compound **6r**) or N-phenyl (compound **6d**) reduced the activity.

Meta COMe substitution at N-phenyl ring (compounds **6r** and **7g**) provided more potent AChE inhibition than *para* position of both series of compounds. *Para* OH substitution at 4-phenyl ring (compounds **6p** and **7d**) or N-phenyl (compound **7k**) showed better AChE inhibition than other substitutions (Cl, and Me) or without substitution (compound **6a**). Substitution of 4-Cl group at N-phenyl (compound **6b**) increased the AChE activity than 3-Cl group (compound **6c**) or without substitution (compound **6a**). *Para* COMe at N-phenyl and 4-OH (compound **7v**) or 4-Cl (compound **7l**) at 4-phenyl moiety of (±) (E)-N-aryl-4-hydroxy-4-phenylbut-2-enamides increased AChE inhibition.

Molecule with OH group at 4-phenyl moiety and 3-quinolinyl (compound **7q**) as amide substitution of (±) (E)-N-aryl-4-hydroxy-4-phenylbut-2-enamides, reduced the BBB permeability, that has unnecessary for CNS targeted drug candidates. Whereas, *para* OH group at N-phenyl (compound **6n**), 4-NO_2 at 4-phenyl ring (compound **6o**) or 4-COMe at N-phenyl with 4-OH group at 4-phenyl ring (compound **6q**) of 4-oxo-N, 4-diphenylbutanamides, diminished the BBB permeability.

5.3.5.6 Cellular cytotoxicity and neuroprotection assessment

The cell viability and neuroprotective potential, against excitotoxicity, of synthesized small molecules, were evaluated on human neuroblastoma SH-SY5Y cell line. Cells were exposed to considerably high concentrations of the test compounds (50μM and

100μM) for 24 h to investigate their cytotoxicity. The cell viability was determined by MTT assay. Selected compounds of both series, showed insignificant cell death even at high concentrations (**Table 5.10**). The neuroprotective potential was assessed by using L-glutamate as excitotoxic agent. In this assay, addition of L-glutamate (100μM) to growth media caused significant cell death as was evidenced by reduction in cell viability. The results (**Table 5.10**) are mean ± SEM of at least three independent experiments.

Table 5.10 Cell viability and neuroprotection of synthesized compounds on SH-SY5Y cell line

Compound	Cell viability (%)[a]		Neuroprotection (%)[b]
	100μM	50μM	25μM
6c	75.76±0.49	92.72±0.35	25.19±0.23
6f	90.2±0.39	96.95±0.08	31.23±0.42
6m	96.81±0.41	99.19±0.09	35.81±0.31
6n	96.40±0.16	99.19±0.21	32.26±0.42
7b	85.46±0.25	94.8±0.49	41.55±0.11
7k	96.58±0.31	98.29±0.24	5.51±0.12
7p	90.89±0.40	96.35±0.32	36.15±0.61

[a]Percentage cell viability of SH-SY5Y cells exposed at relatively high concentrations (50μM and 100μM) of test compounds. [b]Percentage neuroprotection of SH-SY5Y cells at relatively lower concentrations (25μM) of the test compounds against L-glutamate (100μM).

5.3.6 Molecular dynamics simulation

MD simulations of compounds **6m**-AChE, **6n**-MAO-B, **7k**-MAO-B, and **7p**-MMP-9 complexes were performed to establish the binding potency and amino acid residue interactions. RMSD of the protein backbone C-α atoms and individual inhibitor, root mean square fluctuation (RMSF) in the individual amino acid side chain and ligand-protein interactions were recorded throughout 50 ns of MD simulations. The total dynamic energy of inhibitor-protein complexes was stable in last 40 ns of complete

simulations. The temperature, pressure, volume, and potential energy of the complex remained constant during simulations, representing the robustness and reliability of the simulations. The RMSD of simulation converging between 0.4 and 3.5Å indicated the stability of macromolecule with ligands in complexes during 50 ns simulation. The RMSF in individual amino acid residues, during the entire simulation, was below 5.2 Å, representing a lower degree of conformational changes in the side chains. RMSD of protein backbone C-α along with the ligand RMSD values became constant after initial 10 ns simulations. RMSD plot displayed RMSD values for protein on the left Y-axis and ligand on the right Y-axis, protein backbone in green and ligand in maroon. The mean RMSD value for compounds **6m**-AChE (**Figure 5.9**), **6n**-MAO-B (**Figure 5.10**), **7k**-MAO-B (**Figure 5.11**) and **7p**-MMP-9 (**Figure 5.12**) complexes were 1.05, 1.2, 1.8 and 1.6 Å respectively.

RMSF value was helpful for characterizing local changes along the protein chain C-α and peaks denoted the areas of the protein that fluctuate the most during the simulation. RMSF of the complexes were below 4.5 Å, representing fewer fluctuation and better stability of ligand-protein complexes during MD. The simulation study revealed that compound **6m** (**Figure 5.9**) interacted to Phe295 with H-bonding only, whereas Tyr341 amino acid with H-bonding as well as π-π stacking interactions at PAS site of AChE.

Compound **6n** (**Figure 5.10**) bound to Ser200 with only H-bonding, but Tyr326 with H-bonding as well as π-π stacking interactions at the active site of MAO-B. Compound **7k** (**Figure 5.11**) associated with Pro102 by direct H-bonding, but interacted Ile199 and Lys296 amino acids with H-bonding through a water molecule at binding pocket of MAO-B. Compound **7p** (**Figure 5.12**) produced direct hydrogen bonding with Tyr248 and hydrogen bonding through water molecule with Ieu188 residue at active site of MMP-9.

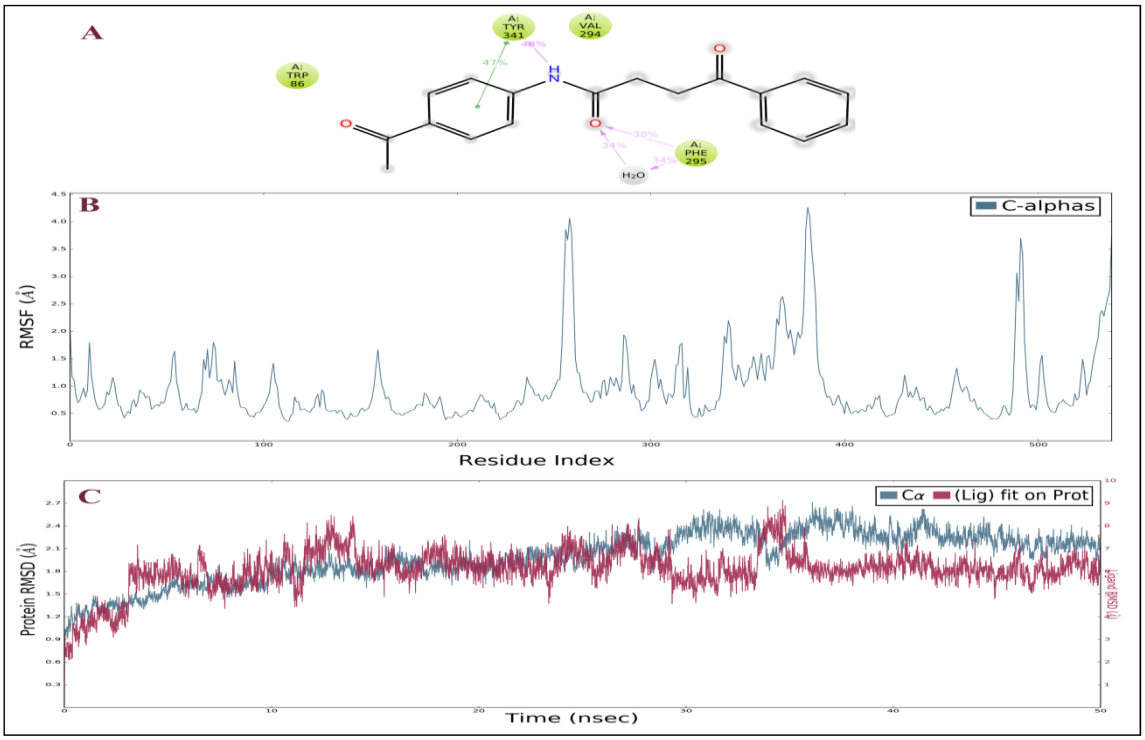

Figure 5.9 MD simulations of compound **6m** with AChE: A, Docking pose after MD; B, RMSF curve for C-alphas; C, protein, and ligand RMSD curve.

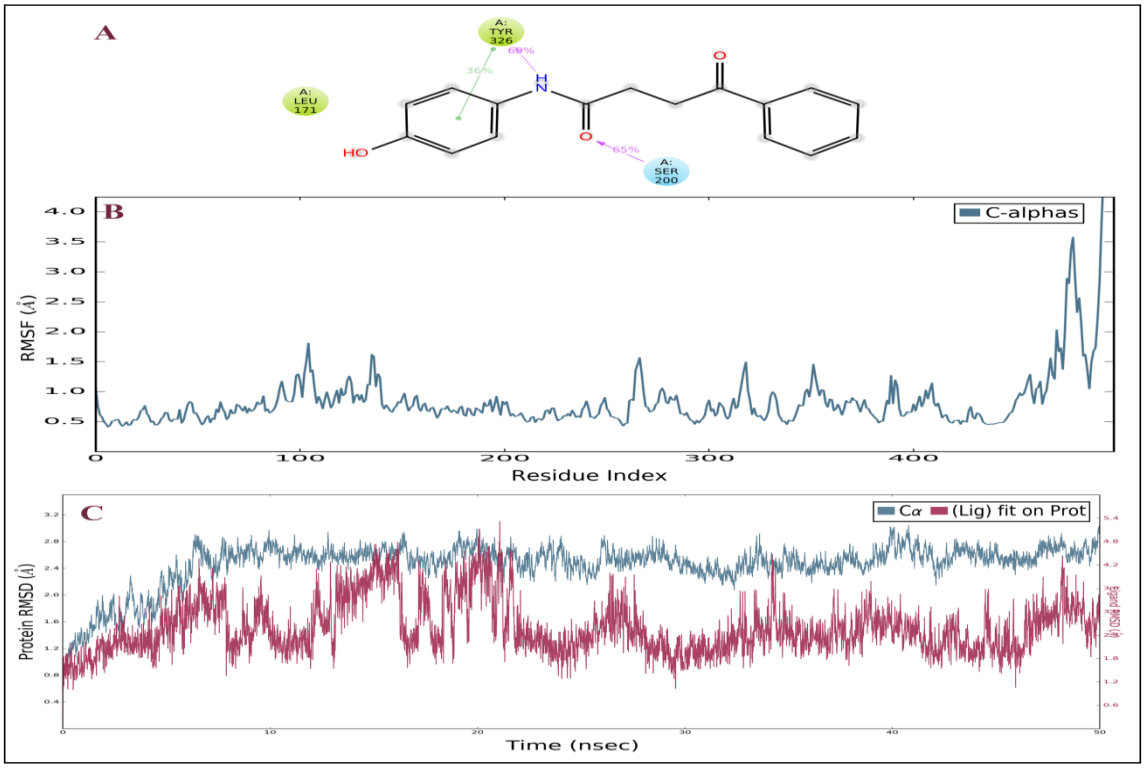

Figure 5.10 MD simulations of compound **6n** with MAO-B: A, Docking pose after MD; B, RMSF curve for C-alphas; C, protein, and ligand RMSD curve.

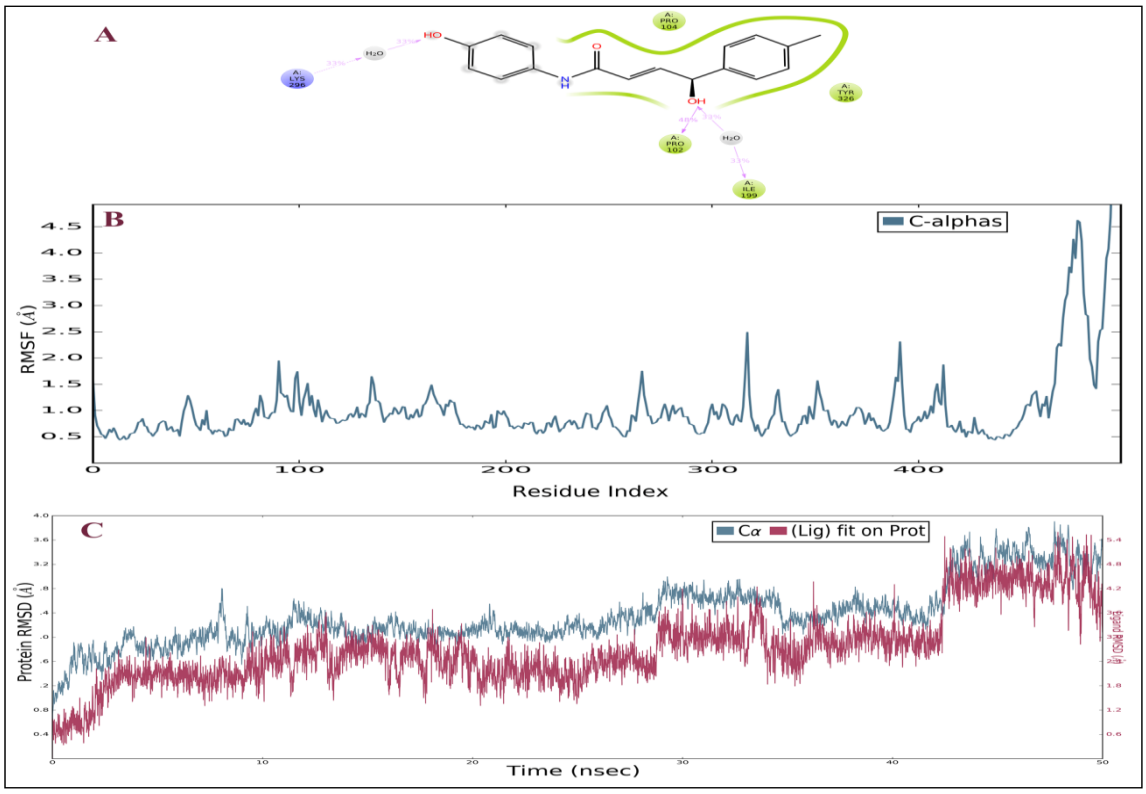

Figure 5.11 MD simulations of compound **7k** with MAO-B: A, Docking pose after MD; B, RMSF curve for C-alphas; C, protein, and ligand RMSD curve.

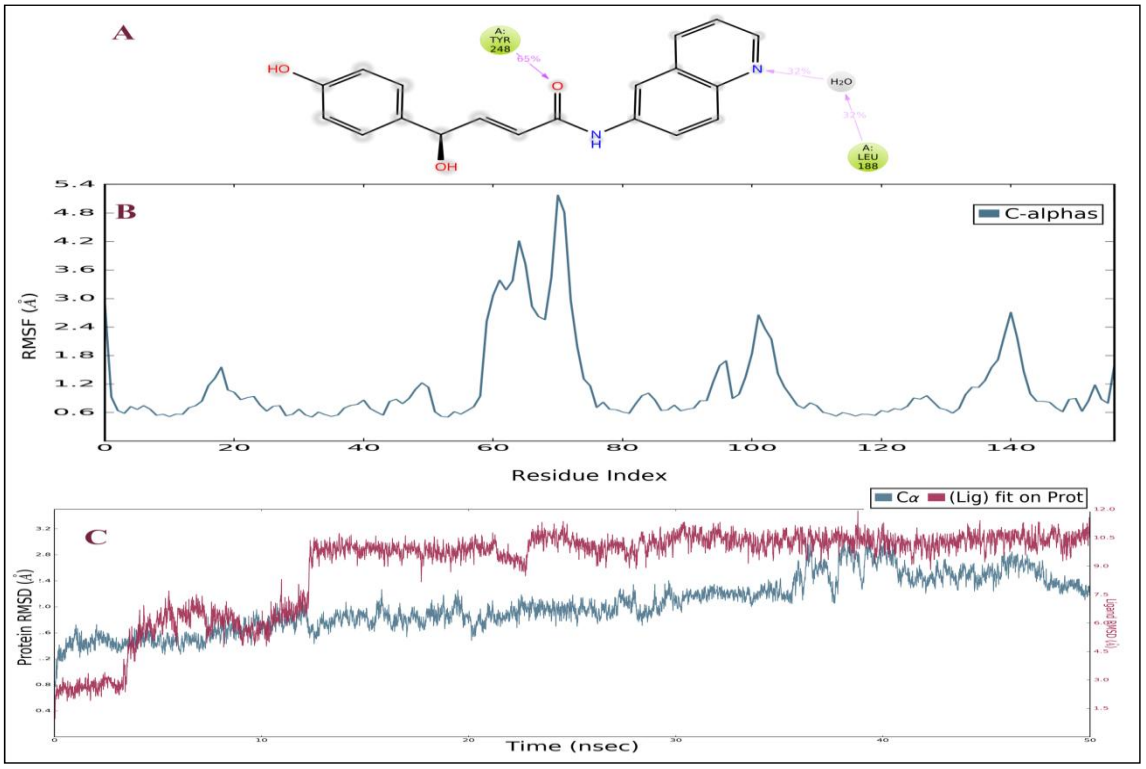

Figure 5.12 MD simulations of compound **7p** with MMP-9: A, Docking pose after MD; B, RMSF curve for C-alphas; C, protein and ligand RMSD curve.

5.4 Conclusions

The fragment-based drug design provided 4-oxo-N, 4-diphenyl butanamides as selective MAO-B inhibitors with cholinesterase inhibition. Compounds **6b**, **6h**, **6j**, **6k, 6m**, **6n**, and **6p** produced better MAO-B inhibition than the rest. Electron withdrawing groups (*e.g.,* CF_3, COMe) at *meta*-position of N-phenyl moiety provided more potent activity as compared to *para*-substitution. Substitution at *para*-position of 4-phenyl ring caused a decrease in the activity. Modification at 4-oxo-butane motif of 4-oxo-N, 4-diphenyl butanamides by 4-hydroxy but-2-ene, resulted in more potent MAO-B inhibition than pargyline. Compounds **7k**, **7s**, **7u**, & **7v** showed potent MAO-B inhibition and compounds **7k**, **7u**, and **7v** also provided AChE inhibition (IC_{50}) within nanomolar range. The synthesized compounds showed remarkable BBB permeability, neuroprotectivity, and no toxicity. Further, the substitution at *para*-position of 4-phenyl moiety with OH group showed better inhibition activity than other groups (H, CH_3, Cl, OMe).

5.5 References

[1] J.C. Shih, Molecular basis of human MAO-A and B, *Neuropsychopharmacology*, 4(1) (1991) 1–7.

[2] A. Bach, N.C. Lan, D.L. Johnson, C.W. Abell, M.E. Bembenek, S.-W. Kwan, P.H. Seeburg, J.C. Shih, cDNA cloning of human liver monoamine oxidase A and B: molecular basis of differences in enzymatic properties, *Proceedings of the National Academy of Sciences*, 85 (1988) 4934–4938.

[3] B. Kumar, A.K. Mantha, V. Kumar, Recent developments on the structure-activity relationship studies of MAO inhibitors and their role in different neurological disorders, *RSC Advances*, 6 (2016) 42660–42683.

[4] R. Adolfsson, C. Gottfries, B. Roos, B. Winblad, Changes in the brain catecholamines in patients with dementia of Alzheimer type, *The British Journal of Psychiatry*, 135 (1979) 216–223.

[5] J. Saura, J. Luque, A. Cesura, M. Da Prada, V. Chan-Palay, G. Huber, J. Löffler, J. Richards, Increased monoamine oxidase B activity in plaque-associated astrocytes of Alzheimer brains revealed by quantitative enzyme radioautography, *Neuroscience*, 62 (1994) 15–30.

[6] M. Weinstock, Selectivity of cholinesterase inhibition, *CNS drugs*, 12 (1999) 307–323.

[7] P.N. Tariot, R.M. Cohen, T. Sunderland, P.A. Newhouse, D. Yount, A.M. Mellow, H. Weingartner, E.A. Mueller, D.L. Murphy, L-deprenyl in Alzheimer's disease: preliminary evidence for behavioral change with monoamine oxidase B inhibition, *Archives of General Psychiatry*, 44 (1987) 427–433.

[8] D.M. Fink, M. Palermo, G.M. Bores, F.P. Huger, B.E. Kurys, M.C. Merriman, G.E. Olsen, W. Petko, G.J. O'Malley, Imino 1, 2, 3, 4-tetrahydrocyclopent [b] indole carbamates as dual inhibitors of acetylcholinesterase and monoamine oxidase, *Bioorganic & Medicinal Chemistry Letters*, 6 (1996) 625–630.

[9] C. Brühlmann, F. Ooms, P.-A. Carrupt, B. Testa, M. Catto, F. Leonetti, C. Altomare, A. Carotti, Coumarins derivatives as dual inhibitors of acetylcholinesterase and monoamine oxidase, *Journal of Medicinal Chemistry*, 44 (2001) 3195–3198.

[10] G.A. Rosenberg, Matrix metalloproteinases and their multiple roles in neurodegenerative diseases, *The Lancet Neurology*, 8 (2009) 205–216.

[11] D.C. Rees, M. Congreve, C.W. Murray, R. Carr, Fragment-based lead discovery, *Nature Reviews Drug Discovery*, 3 (2004) 660–672.

[12] H.M. Berman, J. Westbrook, Z. Feng, G. Gilliland, T.N. Bhat, H. Weissig, I.N. Shindyalov, P.E. Bourne, The protein data bank, *Nucleic Acids Research*, 28 (2000) 235–242.

[13] B.J. Drakulić, T.P. Stanojković, Ž.S. Žižak, M.M. Dabović, Antiproliferative activity of aroylacrylic acids. Structure-activity study based on molecular interaction fields, *European Journal of Medicinal Chemistry*, 46 (2011) 3265–3273.

[14] J. Krall, C.H. Jensen, F. Bavo, C.B. Falk-Petersen, A.S. Haugaard, S.B. Vogensen, Y. Tian, M. Nittegaard-Nielsen, S.B. Sigurdardóttir, J. Kehler, K.T. Kongstad, D.E. Gloriam, R.P. Clausen, K. Harpsøe, P. Wellendorph, B. Frølund, Molecular Hybridization of Potent and Selective γ-Hydroxybutyric Acid (GHB) Ligands: Design, Synthesis, Binding Studies, and Molecular Modeling of Novel 3-Hydroxycyclopent-1-enecarboxylic Acid (HOCPCA) and trans-γ-Hydroxycrotonic Acid (T-HCA) Analogs, *Journal of Medicinal Chemistry*, 60 (2017) 9022–9039.

[15] M. Zhao, W. Li, X. Li, K. Ren, X. Tao, X. Xie, T. Ayad, V. Ratovelomanana-Vidal, Z. Zhang, Enantioselective Ruthenium (II)/Xyl-SunPhos/Daipen-Catalyzed Hydrogenation of γ-Ketoamides, *The Journal of Organic Chemistry*, 79 (2014) 6164–6171.

[16] X. Di, J. Yan, Y. Zhao, J. Zhang, Z. Shi, Y. Chang, B. Zhao, L-theanine protects the APP (Swedish mutation) transgenic SH-SY5Y cell against glutamate-induced excitotoxicity via inhibition of the NMDA receptor pathway, *Neuroscience*, 168 (2010) 778–786.

[17] S.B. Berman, T.G. Hastings, Dopamine oxidation alters mitochondrial respiration and induces permeability transition in brain mitochondria: implications for Parkinson's disease, *Journal of Neurochemistry*, 73 (1999) 1127–1137.

[18] O.H. Lowry, N.J. Rosebrough, A.L. Farr, R.J. Randall, Protein measurement with the Folin phenol reagent, *Journal of Biological Chemistry*, 193 (1951) 265–275.

[19] M. Yáñez, N. Fraiz, E. Cano, F. Orallo, Inhibitory effects of cis-and trans-resveratrol on noradrenaline and 5-hydroxytryptamine uptake and on monoamine oxidase activity, *Biochemical and Biophysical Research Communications*, 344 (2006) 688–695.

[20] M. Zhou, N. Panchuk-Voloshina, A one-step fluorometric method for the continuous measurement of monoamine oxidase activity, *Analytical Biochemistry*, 253 (1997) 169–174.

[21] P.R. Twentyman, M. Luscombe, A study of some variables in a tetrazolium dye (MTT) based assay for cell growth and chemosensitivity, *British Journal of Cancer*, 56 (1987) 279–285.

[22] B. Sameem, M. Saeedi, M. Mahdavi, H. Nadri, F.H. Moghadam, N. Edraki, M.I. Khan, M. Amini, Synthesis, docking study and neuroprotective effects of some novel pyrano [3, 2-c] chromene derivatives bearing morpholine/phenylpiperazine moiety, *Bioorganic & Medicinal Chemistry*, 25 (2017) 3980–3988.

[23] M.R. Berthold, N. Cebron, F. Dill, T. Gabriel, T. Kötter, T. Meinl, P. Ohl, C. Sieb, K. Thiel, B. Wiswedel, KNIME: The Konstanz Information Miner Studies in Classification, Data Analysis, and Knowledge Organisation (GfKL 2007) *Springer*, (2007).

[24] G.A. Kaminski, R.A. Friesner, J. Tirado-Rives, W.L. Jorgensen, Evaluation and reparametrization of the OPLS-AA force field for proteins via comparison with accurate quantum chemical calculations on peptides, *The Journal of Physical Chemistry B*, 105 (2001) 6474–6487.